JACS
JOURNAL OF THE AMERICAN CHEMICAL SOCIETY
Article
pubs.acs.org/JACS

The "Catalytic Nitrosyl Effect": NO Bending Boosting the Efficiency of Rhenium Based Alkene Hydrogenations

Yanfeng Jiang,[†] Birgitta Schirmer,[‡] Olivier Blacque,[†] Thomas Fox,[†] Stefan Grimme,[§] and Heinz Berke*[,†]

[†]Anorganisch-Chemisches Institut, Universität Zürich, Winterthurerstrasse 190, CH-8037, Zürich, Switzerland

[‡]Organisch-Chemisches Institut, Universität Münster, Corrensstrasse 40, 48149 Münster, Germany

[§]Mulliken Center for Theoretical Chemistry, Institut für Physikalische und Theoretische Chemie, Universität Bonn, Beringstrasse 4, D-53115 Bonn, Germany

Supporting Information

ABSTRACT: Diiodo Re(I) complexes $[ReI_2(NO)(PR_3)_2(L)]$ (**3**, L = H_2O; **4** , L = H_2; R = *i*Pr **a**, Cy **b**) were prepared and found to exhibit in the presence of "hydrosilane/$B(C_6F_5)_3$" co-catalytic systems excellent activities and longevities in the hydrogenation of terminal and internal alkenes. Comprehensive mechanistic studies showed an inverse kinetic isotope effect, fast H_2/D_2 scrambling and slow alkene isomerizations pointing to an Osborn type hydrogenation cycle with rate determining reductive elimination of the alkane. In the catalysts' activation stage phosphonium borates $[R_3PH][HB(C_6F_5)_3]$ (**6**, R = *i*Pr **a**, Cy **b**) are formed. VT ^{29}Si- and ^{15}N NMR experiments, and dispersion corrected DFT calculations verified the following facts: (1) Coordination of the silylium cation to the O_{NO} atom facilitates nitrosyl bending; (2) The bent nitrosyl promotes the heterolytic cleavage of the H−H bond and protonation of a phosphine ligand; (3) H_2 adds in a bifunctional manner across the Re−N bond. Nitrosyl bending and phosphine loss help to create two vacant sites, thus triggering the high hydrogenation activities of the formed "superelectrophilic" rhenium centers.

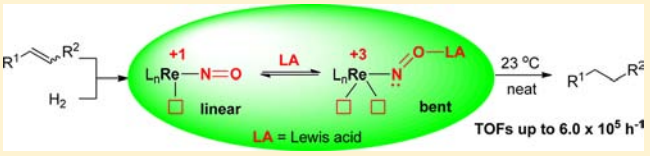

1. INTRODUCTION

The nitrosyl (NO) ligand exhibits noninnocent properties able to switch its binding to metal centers from the linear (three-electron donor) to the bent (one-electron donor) binding mode.[1] The bending of the nitrosyl ligand creates a vacant site accompanied by a formal $2e^-$ oxidation of the metal center without the requirement of preceding ligand dissociation.[2] Such redox change with NO bending, which was termed "stereochemical control of valence" by Enemark and Feltham,[3] gave us the notion that the NO ligand could be used to generate a vacant site "on demand" by bending, which for rhenium as a middle transition element is normally a difficult process, since rhenium shows a great tendency to establish stable 18 electron complexes. Moreover, nitrosyl ligands at electron rich metal centers possess high Lewis basicity at the O_{NO} atom.[4] Interaction with Lewis acids could subsequently increase the metal to NO π-back-donation, which in principle facilitates the NO bending. With regard to Negishi's idea of catalytic enhancement by formation of "super Lewis acids" or "super-electrophiles",[5] the Lewis acid promoted NO bending together with a vacant site generated in the catalytic reaction could be regarded as a "double Lewis acid". However, following this idea, it remained challenging to find an appropriate transition metal nitrosyl system to cooperate with a suitable Lewis acid for amplification of the "nitrosyl effect" and to bring about efficient catalyses. It deserves special mentioning that hydrogenations[6] ranking highest next to C−C coupling catalyses were up to now not documented based on the "catalytic nitrosyl effect".

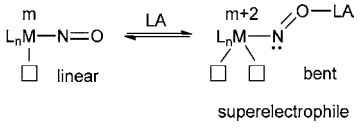

Our group has systematically studied rhenium nitrosyl chemistry, particularly aimed to be applied in reductive catalyses.[7] In continuation of attempts to use ligand tuning to achieve improved catalytic performance, we demonstrated recently that the use of boron Lewis acids as co-catalysts can greatly enhance alkene hydrogenations applying *trans*-diphosphine Re(I) bromo hydrides as catalysts comparable to the performance of platinum group metal complexes.[8] In these cases, reversible bromide abstractions assisted by the external boron Lewis acid were the key activation step. The nitrosyl ligand, on the other hand, functioned in these systems merely as a strongly bound ancillary ligand with strong π-acceptor properties endowing additionally a *trans*-effect or *trans*-influence. Could the NO ligand attribute a still more sophisticated functional role to improve catalysis? This question challenged us to explore the ways of how to enforce NO bending and to utilize it for catalysis.

In this article, we would like to disclose the first example of a "catalytic nitrosyl effect" triggering efficient hydrogenations of alkenes. Our explorations were based on systems of *trans*-diphosphine diiodo Re(I) mononitrosyl complexes modified by

Received: January 9, 2013
Published: February 5, 2013

dx.doi.org/10.1021/ja400135d | *J. Am. Chem. Soc.* 2013, 135, 4088−4102

reactions with silylium cations as Lewis acids (Scheme 1). This work was inspired by two underlying facts: (1) The nucleophilicity of metal bound halogens decreases in the order of F > Cl > Br > I. The weakest nucleophile iodide exhibits least tendency toward attack from an external Lewis acid; (2) The silylium species R'_3Si^{+}[9] generated *in situ* from a $R_3'SiH/B(C_6F_5)_3$ mixture is one of the strongest oxophiles, as exemplified by the work of Piers[10] and Oestreich[11] in hydrosilylations of carbonyl groups. Comprehensive mechanistic studies were carried out to accomplish eventually silylium facilitated nitrosyl bending and of phosphine loss as the key activation steps. Quantum chemical calculations were employed to establish plausibility for the experimentally derived reaction pathways.

Scheme 1

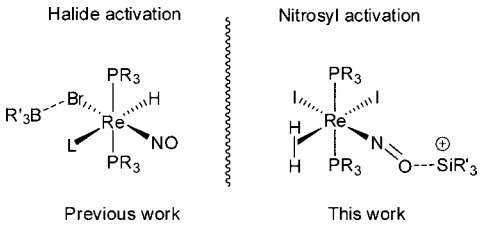

2. RESULTS AND DISCUSSION

2.1. Synthesis and Characterization of Re(I) Mononitrosyl Diiodo Complexes. The Re(I) iodo complexes were prepared either by a one-pot synthesis route starting from rhenium metal or via a Finkelstein type bromide/iodide exchange reaction, as depicted in Scheme 2. Treatment of Re metal with H_2O_2 followed by reduction with H_3PO_2/NO in the presence of NEt_4I/HI afforded a crude deep blue Re(II) iodonitrosyl compound, which was further reacted with excess of PCy_3 in ethanol giving within 15 h at 90 °C a diiodo aqua Re(I) complex $[ReI_2(NO)(PCy_3)_2(H_2O)]$ (**3b**) in 20% overall yield. The presence of an aqua ligand could be assured by the appearance of a broad OH absorption at 3566 cm^{-1} in the IR spectrum and a OH singlet at 5.20 ppm (THF-d_8) which disappeared in the ^1H NMR spectrum upon addition of D_2O. The X-ray crystallographic analysis of **3b** revealed a pseudo-octahedral geometry of the rhenium center with the weak aqua ligand *trans* to the strong NO ligand (Figure 1). Two solvent THF molecules are fixed in the crystal lattice showing intermolecular hydrogen bonding to the aqua ligand possessing protons acidified by coordination of the H_2O molecule. The two iodo ligands are located *trans* revealing a slight bending toward the aqua ligand (I1−Re1−I2 = 169.390(9)°). A relatively high electron density at the rhenium center, which is enhanced by the strong π donation of the iodide ligands, causes a low NO IR stretching frequency at 1664 cm^{-1}. The low overall yield of **3b** is assumed to be caused by decomposition of the hydroiodic acid in the reduction step. To overcome this disadvantage, an alternative Re(II) bromonitrosyl precursor was employed applying a Finkelstein type exchange reaction to introduce the iodo ligands. Treatment of $[NEt_4]_2[ReBr_5(NO)]$ with excess of NaI in THF afforded at 90 °C within 24 h a crude deep blue Re(II) product. Single crystals were obtained from THF/Et_2O and X-ray diffraction revealed a $[NEt_4][trans\text{-}ReI_4(NO)(THF)]$ structure (see Supporting Information). Treatment of this crude precursor with excess of PCy_3 in a mixture of ethanol and water furnished the formation of pure **3b** in an overall yield of 67% (Scheme 2).

Scheme 2. Synthesis of Re(I) Mononitrosyl Diiodo Complexes

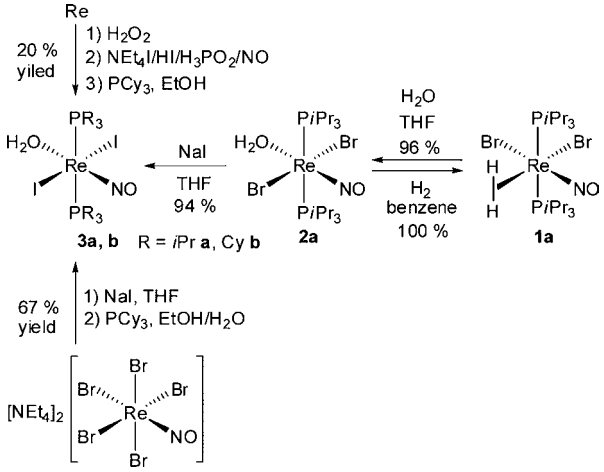

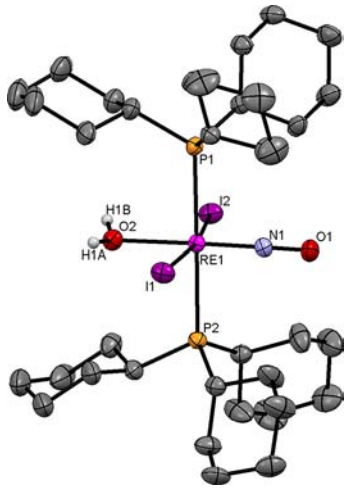

Figure 1. Molecular structure of $[ReI_2(NO)(PCy_3)_2(H_2O)]$ (**3b**) with two THF molecules with 50% probability displacement ellipsoids. All hydrogen atoms were omitted for clarity except for the H_2O ligand. Selected bond lengths (Å) and angles (deg): P(1)−Re(1), 2.5389(10); P(2)−Re(1), 2.5198(10); I(1)−Re(1), 2.7589(3); I(2)−Re(1), 2.7653(2); N(1)−Re(1), 1.7335(34); N(1)−O(1), 1.1994(42); O(2)−Re(1), 2.1733(24); N(1)−Re(1)−O(2), 178.98(11); P(2)−Re(1)−P(1), 179.23(3); I(1)−Re(1)−I(2), 169.390(9); O(1)−N(1)−Re(1), 179.3(3).

We found that the above approach could not be applied to the P*i*Pr$_3$ congener as large amounts of $[HPiPr_3]I$ were formed in the last synthetic step. Therefore, we resorted to another route using the Re(I) dibromo dihydrogen complex $[ReBr_2(NO)(PiPr_3)_2(\eta^2\text{-}H_2)]$ (**1a**) as a starting material. In THF solution, the η^2-H_2 ligand of **1a** could be replaced by H_2O at 90 °C within 5 min affording the aqua complex $[ReBr_2(NO)(PiPr_3)_2(H_2O)]$ (**2a**) in quantitative yield. The IR spectrum showed a broad ν(OH) absorption at 3428 cm^{-1} and a strong ν(NO) band at 1667 cm^{-1}. The ^1H NMR spectrum displayed a singlet resonance at 5.72 ppm in THF-d_8 for the aqua ligand. Like for the iodo analogue, a single-crystal X-ray diffraction

dx.doi.org/10.1021/ja400135d | J. Am. Chem. Soc. 2013, 135, 4088−4102

study of **2a** revealed *trans* alignment of the aqua molecule and the nitrosyl ligand (see Supporting Information). The transformation from **1a** to **2a** was reversible. In H_2 atmosphere, **1a** was recovered instantaneously in quantitative yield from **2a** in benzene solution. The double *cis* labilization effect of the two bromides and the *trans* effect of NO were expected to labilize the aqua ligand so much that for instance double halogen anion exchange would become accessible via exchange with the labile water ligand position. Indeed, treatment of **2a** with excess of NaI in THF afforded within 2 h at room temperature the diiodo aqua Re(I) congener $[ReI_2(NO)(PiPr_3)_2(H_2O)]$ (**3a**) in 94% isolated yield. The IR spectra showed a broad ν(OH) absorption at 3434 cm^{-1}. The NO stretching frequency is observed at 1674 cm^{-1}, which is close to those of **2a** and **3b**. In the ^1H NMR spectra the aqua ligand appeared as a singlet at 5.43 ppm in THF-d_8. The $^{31}P\{^1H\}$-NMR spectrum exhibited a singlet at −10.7 ppm shifted relatively high-field.

The aqua ligand in **3a,b** is labile due to the strong *cis* labilization effect of the two iodides. Under 1 bar of H_2 in benzene, the aqua ligand could be instantaneously replaced by η^2-H_2 at 23 °C to afford the dihydrogen complexes $[ReI_2(NO)(PR_3)_2(\eta^2\text{-}H_2)]$ (**4**, R = *i*Pr **a**, Cy **b**,) in 100% *in situ* yields (Scheme 3). The $^{31}P\{^1H\}$-NMR spectra displayed a singlet at δ

Scheme 3. Reaction of 3 with H_2 and CO

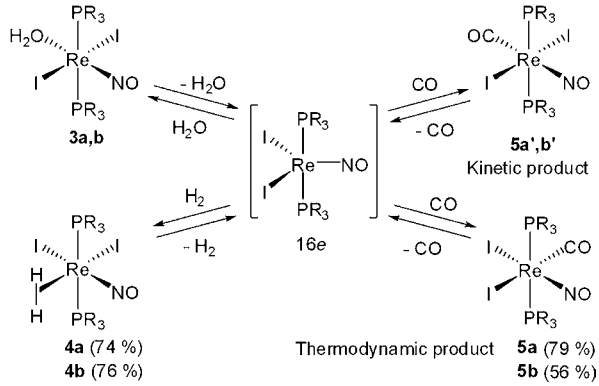

3.06 (**4a**) or −4.94 ppm (**4b**). The ^1H NMR spectra exhibited triplet signals for the η^2-H_2 ligand at 0.64 ppm (**4a**, $^2J_{(HP)}$ = 20 Hz, T_1 = 98 ms, THF-d_8) and 0.80 ppm (**4b**, $^2J_{(HP)}$ = 21 Hz, T_1 = 42 ms, benzene-d_6), which are both shifted high-field compared to those of **1a** and **1b** implying a strong electron shielding effect. The relatively long T_1 time of **4a,b** indicates an elongated H_2 ligand approaching a dihydride structure. This verifies the geometry of **4a,b** bearing *cis*-aligned H_2 and NO ligands. A η^2-H_2 *trans* to NO is expected to exhibit a T_1 time less than 10 ms corresponding to a classical dihydrogen character due to the competition between the σ^*_{HH} and π^*_{NO} orbitals for back-bonding. Pure solid **4a,b** could be obtained in 74% (**4a**) and 76% (**4b**) yield, respectively, from the same reaction, but required the presence of anhydrous $MgSO_4$, which helped to trap the liberated H_2O and prevented the back-reaction to **3a,b** during solvent evaporation. The IR spectra showed strong ν(NO) absorptions at 1719 (**4a**) and 1710 cm^{-1} (**4b**). The reaction course from **3** to **4** can be interpreted in terms of the initial formation of the 16e intermediate $[ReI_2(NO)(PR_3)_2]$, which is assumed to be stabilized by the two strong π-donating and strongly *cis*-labilizing iodides. Dihydrogen, as a weak σ-donor and a good π-acceptor, places itself preferentially between I and NO leading to the thermodynamically most stable **4a,b** species. The assumed kinetic product with H_2 *trans* to the nitrosyl could not be observed by NMR spectroscopy presumably due to the fact that the π acceptor H_2 is electronically too activated *trans* to NO.

Interestingly, the reaction of **3a,b** or **4a,b** with CO allows the trapping of kinetic products. Treatment of either **3a,b** or **4a,b** with 1 bar of CO in benzene-d_6 at 23 °C afforded instantaneously the kinetic product $[ReI_2(PR_3)_2$-*trans*-(NO)-(CO)] (**5′**, R = *i*Pr **a**, Cy **b**) in 100% *in situ* yield originating from CO attack between the two iodides of the $16e^-$ $[ReI_2(NO)(PR_3)_2]$ species. The IR spectra showed strong ν(CO) absorptions at unexpectedly high wavenumbers (2082 for **5a′** and 2074 cm^{-1} for **5b′**) indicating a high CO electrophilicity. A singlet resonance at δ −16.7 ppm (**5a′**) or −26.3 (**5b′**) was observed in the $^{31}P\{^1H\}$-NMR spectra. **5a′,b′** is unstable mainly due to the strong π-acceptors CO and NO *trans* to each other. Therefore, CO attack between iodide and NO is taking place which is apparently kinetically hindered and slow, leading to the thermodynamically stable complex $[ReI_2(NO)(CO)(PR_3)_2]$ (**5**, R =*i*Pr **a**, Cy **b**) within 15 h at 23 °C. In comparison with **5a′,b′**, the $^{31}P\{^1H\}$-NMR signals were shifted low-field to δ −6.5 (**5a**) and −14.5 ppm (**5b**) and the CO stretching frequencies became red-shifted to 1969 (**5a**) and 1970 cm^{-1} (**5b**) with respect to the ν(NO) absorption at 1723 cm^{-1} for **5a** and 1712 cm^{-1} for **5b**. An X-ray diffraction study of **5b** confirmed the molecular structure with two *cis*-iodides, and the NO and CO ligands *cis* positioned (Figure 2).

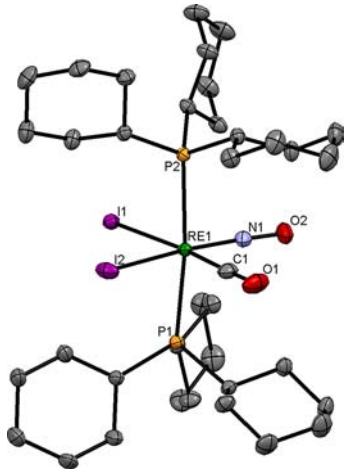

Figure 2. Molecular structure of $[ReI_2(NO)(PCy_3)_2(CO)]$ (**5b**) with 50% probability displacement ellipsoids. Hydrogen atoms have been omitted for clarity. Selected bond lengths (Å) and angles (deg): P(1)−Re(1), 2.5343(4); P(2)−Re(1), 2.5384(4); I(1)−Re(1), 2.81659(13); I(2)−Re(1), 2.78172(15); N(1)−O(2), 1.1805(19). P(1)−Re(1)−P(2), 172.613(13); Re(1)−N(1)−O(2), 173.25(15); I(1)−Re(1)−I(2), 92.52(1).

The coordination geometry of the kinetic and thermodynamic product from the reaction of **3a,b** with H_2 were investigated further by modeling $ReI_2(NO)(PMe_3)_2(\eta^2\text{-}H_2)$ with dispersion corrected DFT. For this purpose the structures were optimized at TPSS-D3/def2-TZVP level.[12−14] Subsequent single-point calculations with the more accurate B2PLYP-D3[15] double hybrid functional and the same basis set yielded the energy values show in Figure 3 (for further details see the Experimental Section and Supporting Information). As shown in Figure 3, the thermodynamic product **II** reveals a η^2-H_2

dx.doi.org/10.1021/ja400135d | J. Am. Chem. Soc. 2013, 135, 4088−4102

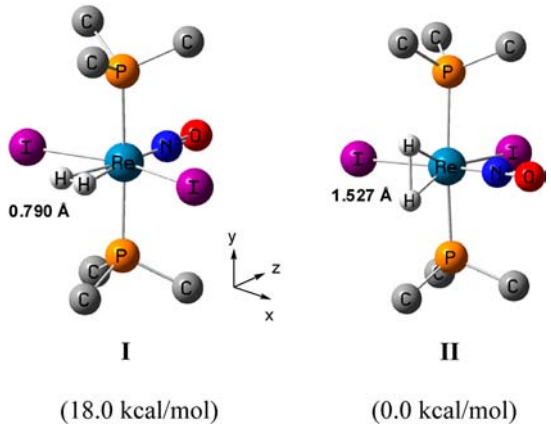

Figure 3. Kinetic and thermodynamic coordination isomers of $[ReI_2(NO)(PMe_3)_2(\eta^2\text{-}H_2)]$ as calculated with B2PLYP-D3/def2-TZVP//TPSS-D3/def2-TZVP. **I**: H−H eclipses I−Re−I axis with *trans*-diiodide. **II**: H−H eclipses P−Re−P axis with *cis*-diiodide ligands. All carbon and hydrogen atoms except for the H_2 ligand are omitted for clarity.

ligand parallel to the P−Re−P axis with a H−H distance of 1.527 Å emphasizing a "compressed" dihydride structure.[16] In comparison, the η^2-H_2 ligand in the kinetic product **I**, which turned out to be a local energy minimum, was found to be perpendicular to the P−Re−P axis and in-plane with the I−Re−I axis exhibiting a H−H bond distance of 0.790 Å corresponding to classical dihydrogen ligand. Importantly, the energy difference between **II** and **I** was determined to be 18.0 kcal/mol in favor of **II** confirming the instability of the geometry of the two π-acceptors of H_2 and NO in *trans* position.[17] The Re−H distance of 2.005 Å in **I** indicates weakness of the H_2 binding to the rhenium center. In contrast, the Re−H distance of 1.662 Å in **II** shows strong bonding between the H atoms and the rhenium. The *trans*-alignment of the strong iodo π-donor and the π-acceptor NO is preferred due to the π "push-pull" interaction.[18]

2.2. Hydrogenation of Alkenes Catalyzed by the "Re(I) Diiodide/Hydrosilane/$B(C_6F_5)_3$" System. The potential of **3a,b** in the catalytic hydrogenation of alkenes was explored. At 90 °C under 10 bar of H_2, **3a,b** showed reasonable activities in the hydrogenation of 1-hexene giving a TON of 1.0×10^4 within 120 min. We reckoned that the catalytic performance of **3a,b** could still be improved by finding ways to facilitate the generation of open sites. Indeed, under milder conditions such as 23 °C, hydrogenation did not occur at all, and this we attributed to the unavailability of open sites. Therefore, utilizing the strong oxophilicity of silicon,[9−11] we envisaged to employ the hydrosilane and $B(C_6F_5)_3$ system as a cocatalyst to generate *in situ* silylium ions expected to attach to the O_{NO} atoms. These NO derivatized species were thought to show facile bending at the N atom with opening of a coordination site.

Indeed, the "Re(I) iodo complex/hydrosilane/$B(C_6F_5)_3$" system was found to exhibit up-to-date the best catalytic performance in hydrogenations under mild conditions ever studied before. To compare the efficiency of different catalytic systems, the prototypic 1-hexene (2.5 mL) hydrogenations were carried out under 10 bar H_2 at 23 °C with a substrate-to-catalyst ratio (S/C) of 10 000. The molar ratio of the rhenium catalyst and the co-catalyst was set to 1:5 with a 1:1 molar ratio of hydrosilane and $B(C_6F_5)_3$. The results are listed in Table 1. The "**3a**/Et_3SiH/$B(C_6F_5)_3$" system revealed a conversion of 92% within 15 min corresponding to a TON of 9200 and TOF of 3.7×10^4 h^{-1}. Full conversion could be reached after 30 min. Further increase of the S/C ratio to 40 000 afforded a TON of 2.0×10^4 and a TOF of 2.7×10^4 h^{-1} within 25 min. In comparison, the two-component systems "**3a**/Et_3SiH" and "**3a**/$B(C_6F_5)_3$" proved to be not catalytically active under the same conditions. Similarly, applying "**3b**/Et_3SiH/$B(C_6F_5)_3$" a TON of 9100 and a TOF of 3.6×10^4 h^{-1} within 15 min were reached corresponding to a 91% conversion. The longevity of the current system is dependent on both the kind of the Lewis acid and of the hydrosilane. With either a "**3a**/Et_3SiH/BPh_3" or a "**3a**/Et_3SiH/AlF_3" system, decrease of the catalytic performance was observed showing low TONs after 5 min. The influence of the hydrosilane on the catalytic performance was studied using the "**3a**/$B(C_6F_5)_3$" system.[19] In the case of sterically more congested hydrosilanes, such as Ph_3SiH and iPr_3SiH, hydrogenation could not be observed. With the medium-sized hydrosilane $MePh_2SiH$, a moderate activity with a TOF of 7750 h^{-1} was seen within 1 h. In the case of the sterically less hindered Me_2PhSiH, which is known to be a better hydride donor than Et_3SiH, improved performance could be achieved. The "**3a**/Me_2PhSiH/$B(C_6F_5)_3$" system brought about a 90% conversion within 7.5 min corresponding to a TON of 9040 and a TOF of 7.2×10^4 h^{-1}. The catalytic system of "**3b**/Me_2PhSiH/$B(C_6F_5)_3$" was even more efficient affording a 93% conversion within 6.5 min corresponding to a TOF of 8.6×10^4 h^{-1}. Noteworthy is the fact that under 40 bar of H_2 at 23 °C the hydrogenations of 1-hexene catalyzed by "**3a,b**/Me_2PhSiH/$B(C_6F_5)_3$" were extremely efficient that over 99% conversions were achieved within 1 min affording the up-to-date highest TOFs of up to 6.00×10^5 h^{-1} (entries 42 and 43 in Table 1).

In general, the catalytic systems of "**3a,b**/Me_2PhSiH/$B(C_6F_5)_3$" were found to be superior to the previously reported "Re(I) bromo hydride/$B(C_6F_5)_3$" system with respect to both activity and longevity. Additionally, it should be pointed out that short induction periods were invariably seen with the "**3a,b**/hydrosilane/$B(C_6F_5)_3$" systems. In comparison, when the dihydrogen derivatives **4a,b** were tested under the same conditions, slightly improved catalytic results were obtained. The "**4a**/Me_2PhSiH/$B(C_6F_5)_3$" system afforded a 97% conversion within 7 min corresponding to a TON of 9700 and a TOF of 8.3×10^4 h^{-1}. With the "**4b**/Me_2PhSiH/$B(C_6F_5)_3$" system, a conversion of 89% was found within 6 min giving a high TOF of 8.8×10^4 h^{-1}, and full conversion was reached within 25 min. Remarkably, induction periods were not noticeable in the **4a,b** cases, which not only verified the initial formation of **4a,b** in "**3a,b**/hydrosilane/$B(C_6F_5)_3$"-catalyzed hydrogenations, but also indicated the negative influence of the aqua molecule in the generation of catalytically active species. Differences in the performance of **3a,b** and **4a,b** became more apparent when "Et_3SiH/$B(C_6F_5)_3$" was applied as a cocatalyst. While a reaction time of 15 min was needed for a 92% conversion based on the "**3a**/Et_3SiH/$B(C_6F_5)_3$" system, the same reaction catalyzed by the "**4a**/Et_3SiH/$B(C_6F_5)_3$" system afforded a conversion of 96% within 10 min corresponding to a TON of 9640 and a TOF of 5.8×10^4 h^{-1} showing again no induction period. Similarly, the hydrogenation of 1-hexene co-catalyzed by "$MePh_2SiH$/$B(C_6F_5)_3$" could also be improved with **4a** giving a TOF of 1.3×10^4 h^{-1} within 30 min.

With terminal alkenes, such as 1-octene, an excellent conversion of 98% was achieved by addition of only 0.0125 mol % of "**3a**/Me_2PhSiH/$B(C_6F_5)_3$" at 23 °C requiring a

dx.doi.org/10.1021/ja400135d | J. Am. Chem. Soc. 2013, 135, 4088−4102

Table 1. Hydrogenation of Alkenes Catalyzed by "[Re]/Hydrosilane/$B(C_6F_5)_3$" Systems[a]

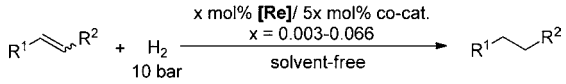

entry	alkene (mmol)	[Re]	co-catalyst	temp (°C)	T (min)	conv (%)	TON	TOF (h^{-1})
1	1-hexene (20)	**3a**	-	23	60	--	--	--
2	1-hexene (20)	**3a**	--	90	120	100	1.0×10^4	5000
3	1-hexene (20)	**3b**	--	90	70	100	1.0×10^4	8571
4	1-hexene (20)	**3a**	$Et_3SiH/B(C_6F_5)_3$	23	15	92	9200	3.7×10^4
5	1-hexene (20)	**3a**	$Et_3SiH/B(C_6F_5)_3$	23	30	100	1.0×10^4	2.0×10^4
6[b]	1-hexene (40)	**3a**	$Et_3SiH/B(C_6F_5)_3$	23	25	50	2.0×10^4	4.9×10^4
7	1-hexene (20)	**3a**	Et_3SiH	23	20	--	--	--
8	1-hexene (20)	**3a**	$B(C_6F_5)_3$	23	20	--	--	--
9	1-hexene (20)	**3a**	Et_3SiH/BPh_3	23	3	5	513	1.0×10^4
10	1-hexene (20)	**3b**	Et_3SiH/BPh_3	23	3	6	658	1.3×10^4
11	1-hexene (20)	**3a**	Et_3SiH/AlF_3	23	5	25	2478	3.0×10^4
12	1-hexene (20)	**3a**	$iPr_3SiH/B(C_6F_5)_3$	23	60	--	--	--
13	1-hexene (20)	**3a**	$Ph_3SiH/B(C_6F_5)_3$	23	40	--	--	--
14	1-hexene (20)	**3a**	$MePh_2SiH/B(C_6F_5)_3$	23	60	78	7750	7750
15	1-hexene (20)	**3a**	$MePh_2SiH/B(C_6F_5)_3$	23	75	90	9040	7.2×10^4
16	1-hexene (20)	**3b**	$MePh_2SiH/B(C_6F_5)_3$	23	65	93	9330	8.6×10^4
17	1-octene (16)	**3a**	$MePh_2SiH/B(C_6F_5)_3$	23	90	98	7812	5208
18	styrene (9)	**3a**	$MePh_2SiH/B(C_6F_5)_3$	23	20	28	1272	3816
19	1,7-octadiene (7)	**3a**	$MePh_2SiH/B(C_6F_5)_3$	90	8	59	4107[c]	3.1×10^4
20	allylcydohexene (6.5)	**3a**	$MePh_2SiH/B(C_6F_5)_3$	90	900	84[d]	2730	182
21	cyclooctene (8)	**3a**	$MePh_2SiH/B(C_6F_5)_3$	23	3	10	402	8036
22	cydooctene (8)	**3a**	$MePh_2SiH/B(C_6F_5)_3$	90	3	65	2611	5.2×10^4
23	cyclooctene (8)	**3b**	$MePh_2SiH/B(C_6F_5)_3$	90	6	38	1540	1.5×10^4
24	cyclohexene (20)	**3a**	$MePh_2SiH/B(C_6F_5)_3$	23	3	3	312	6250
25	cydohexene (20)	**3a**	$MePh_2SiH/B(C_6F_5)_3$	90	30	74	7346	1.5×10^4
26	cyclohexene (20)	**3b**	$MePh_2SiH/B(C_6F_5)_3$	90	20	29	2931	8793
27	1,5-cyclooctadiene (8)	**3a**	$MePh_2SiH/B(C_6F_5)_3$	90	30	84	6696[c]	1.3×10^4
28	1,5-cyclooctadiene (8)	**3b**	$MePh_2SiH/B(C_6F_5)_3$	90	10	20	1629[c]	9776
29	1-hexene (20)	**4a**	--	90	110	97	9710	5296
30	1-hexene (20)	**4b**	--	90	65	99	9940	9175
31	1-hexene (20)	**4a**	$Et_3SiH/B(C_6F_5)_3$	23	10	96	9640	5.8×10^4
32	1-hexene (20)	**4b**	$Et_3SiH/B(C_6F_5)_3$	23	12.5	92	9241	4.4×10^4
33	1-hexene (20)	**4b**	$Et_3SiH/B(C_6F_5)_3$	23	25	100	1.0×10^4	2.4×10^4
34	1-hexene (20)	**4a**	$Me_2PhSiH/B(C_6F_5)_3$	23	7	97	9700	8.3×10^4
35	1-hexene (20)	**4b**	$Me_2PhSiH/B(C_6F_5)_3$	23	6	89	8840	8.8×10^4
36	1-hexene (20)	**4b**	$Me_2PhSiH/B(C_6F_5)_3$	23	25	100	1.0×10^4	2.4×10^4
37	1-hexene (20)	**4a**	$Me_2PhSiH/B(C_6F_5)_3$	23	30	66	6652	1.3×10^4
38	1-octene (16)	**4a**	$Me_2PhSiH/B(C_6F_5)_3$	23	20	50	3982	1.2×10^4
39	styrene (9)	**4a**	$Me_2PhSiH/B(C_6F_5)_3$	23	30	42	1893	3786
40	cyclooctene (8)	**4a**	$Me_2PhSiH/B(C_6F_5)_3$	23	3	9	325	6500
41	cyclooctene (8)	**4a**	$Me_2PhSiH/B(C_6F_5)_3$	90	4	40	1623	2.4×10^4
42[e]	1-hexene (20)	**3a**	$Me_2PhSiH/B(C_6F_5)_3$	23	1	100	1.0×10^4	6.0×10^5
43[e]	1-hexene (20)	**3b**	$Me_2PhSiH/B(C_6F_5)_3$	23	1	99	9900	5.9×10^5

[a]Reactions were performed using 0.002 mmol [Re], 0.01 mmol of hydrosilane, 0.01 mmol of Lewis acid under 10 bar H_2 unless otherwise stated and monitored by a Buechi Pressflow controller. [b]A total of 5 mL of 1-hexene with 0.001 mmol **3a**. [c]Based on the consumption of H_2, as 2 equiv of H_2 was needed for full hydrogenation. [d]Determined by GC–MS spectroscopy. [e]Under 40 bar of H_2.

reaction time of 90 min. The hydrogenation of styrene also worked well under the same conditions affording a TON of 1272 within 20 min. In the case of internal alkenes, such as cyclohexene, cyclooctene (COE), and 1,5-cyclooctadiene (COD), the hydrogenations at 23 °C showed poorer performance presumably due to a relative faster deactivation of the catalysts. For instance, in the hydrogenation of COE catalyzed by 0.025 mol % of "**3a**/$Me_2PhSiH/B(C_6F_5)_3$" deactivation of the catalyst occurred within 3 min giving a TON of 402. Increasing the temperature to 90 °C resulted in improved TONs and TOFs. For instance, while the hydrogenation of cyclohexene catalyzed by the "**3a**/$Me_2PhSiH/B(C_6F_5)_3$" system afforded a low TON value of 312 at 23 °C, the same reaction carried out at 90 °C afforded a TON of 7366 and a TOF of 1.5×10^4 h^{-1} within 30 min. It is interesting to compare the performance of COE with COD as substrates in hydrogenations under 10 bar of H_2 at 90 °C. In terms of activity, the catalysis of COE hydrogenation was found superior with respect to COD giving a higher TOF of 5.2×10^4 h^{-1} within 3 min. In terms of longevity of the catalyst, however,

dx.doi.org/10.1021/ja400135d | J. Am. Chem. Soc. 2013, 135, 4088–4102

COD is a better substrate than COE affording a high TON of 6696 within 30 min. This result not only excluded the alkene coordination step as rate determining, but also suggested the existence of an active species bearing two vacant sites that could be more efficiently stabilized by the bidentated ligand COD than the monodentate COE.

2.3. Mechanistic Studies. *2.3.1. Removal of a PR_3 Ligand via Formation of $[R_3PH][HB(C_6F_5)_3]$ for Catalyst Activation.* It is interesting to note that after catalytic reactions of Table 1 oils had formed. To identify the composition of these oils, we exemplarily scaled up the catalyst loading of "**3a**/Et_3SiH/$B(C_6F_5)_3$" in the hydrogenation of 1-hexene. A precipitate could be isolated and identified by NMR spectroscopy, which turned out to be a mixture with the phosphonium borate $[iPr_3PH][HB(C_6F_5)_3]$ (**6a**) as the main component. In the ^1H NMR spectra, a doublet of quartet signal was observed at 5.62 ppm ($^3J_{HH}$ = 4 Hz, $^1J_{HP}$ = 458 Hz), which was assigned to the $[iPr_3PH]^+$ proton. The ^{11}B NMR spectra exhibited a doublet at −25.4 ppm ($^1J_{BH}$ = 92 Hz), which could be attributed to the $[HB(C_6F_5)_3]^-$ anion. The $^{31}P\{^1H\}$-NMR spectrum showed a unique singlet at 43.9 ppm. In the ^{19}F NMR spectra, the $[HB(C_6F_5)_3]^-$ anion was identified by a set of resonances at −133.40 (m, 6F, *ortho*-C_6F_5), −163.54 (t, $^1J_{CF}$ = 19 Hz, 3F, *para*-C_6F_5) and −166.64 ppm (m, 6F, *meta*-C_6F_5). The presence of free $B(C_6F_5)_3$ was also observed. ESI-MS spectroscopy confirmed the formation of the $[iPr_3PH]^+$ cation (m/z 161.0) and of the $[HB(C_6F_5)_3]^-$ anion (m/z 513.0). It is important to note that the related salt $[HPiPr_3]I$, which could be distinguished from **6a** by its lower solubility in aprotic solvents, was not formed in the resultant solution. Remarkably, when the same hydrogenation reaction was terminated by removing the H_2 atmosphere shortly after the induction period, **6a** was present, as well. The supernatant solution was additionally examined by ^{31}P NMR spectroscopy indicating formation of a minor, yet unknown phosphorus-containing species. By addition of 1-hexene to this solution, hydrogenation could not be initiated suggesting decomposition of the catalytically active species. Similar results were obtained with the catalytic system of "**3b**/$Et_3SiH/B(C_6F_5)_3$" confirming the formation of $[Cy_3PH][HB(C_6F_5)_3]$ (**6b**) as the major phosphorus-containing species after workup of the hydrogenation catalysis. An X-ray crystallographic study of **6b** confirmed the proposed phosphonium borate structure, as shown in Figure 4. Examining other active systems, such as "**3a**(**b**)/$Me_2PhSiH/B(C_6F_5)_3$" and "**4a**(**b**)/$MePh_2SiH/B(C_6F_5)_3$", the formation of **6a** or **6b** was also recognized during and after the hydrogenation experiments.

Figure 4. Molecular structure of $[Cy_3PH][HB(C_6F_5)_3]$ (**6b**) with 30% probability displacement ellipsoids. All hydrogen atoms have been omitted for clarity except for the HB and HP.

To establish the pathway to **6** in more detail, various additional experiments were carried out, as depicted in Scheme 4: (1) The reaction of free $PiPr_3$ or PCy_3 with $B(C_6F_5)_3$ under

Scheme 4. Investigation on the course of the formation of 6

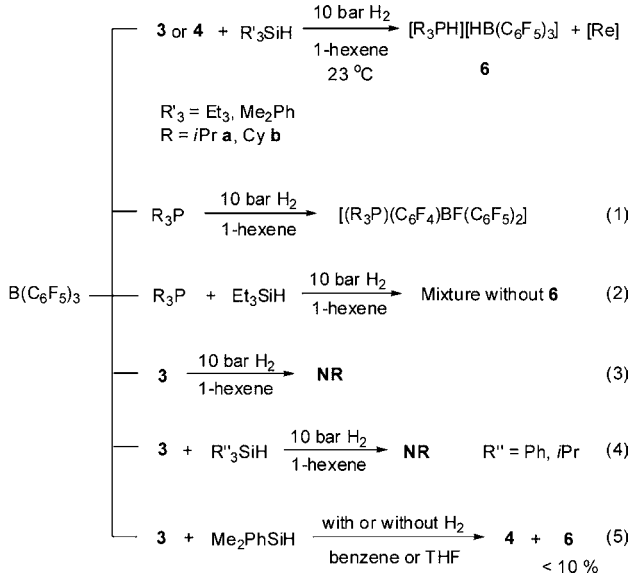

10 bar H_2 in 1-hexene afforded at 23 °C within 10 min the fluoride migrated product $[(R_3P)(C_6F_4)BF(C_6F_5)_2]$ (R = *i*Pr, Cy), which was reported by Stephan et al. to be also accessible via the direct mixing of PR_3 (R = *i*Pr, Cy) with $B(C_6F_5)_3$ in absence of H_2 and alkene.[20] As **6a**,**b** could not be observed from free phosphine and $B(C_6F_5)_3$, a mechanism involving initial dissociation of PR_3 from rhenium and subsequent heterolytic splitting of H_2 by FLPs was excluded.[21] (2) In the absence of **3a**, a mixture of $PiPr_3$ and $B(C_6F_5)_3$ reacts with Et_3SiH in pentane under 10 bar of H_2. However, **6a** was not formed under these circumstances. (3) In absence of Et_3SiH, the reaction of **3a** with $B(C_6F_5)_3$ and H_2 pressure did not afford any precipitate. Likewise, the hydrogenation of 1-hexene catalyzed by **3a**,**b** with no co-catalysts added, did not lead to formation of **6a**,**b**. (4) In the case of an inactive catalytic system, such as "**3a**/$B(C_6F_5)_3$" with either iPr_3SiH or Ph_3SiH, **6a** was also not formed. These results implied that the phosphonium borate was generated in the course of the catalyst's activation. (5) The alkene proved to be not an essential reaction component, since **6a** could still be generated along with the formation of **4a** from a mixture of **3a**, $B(C_6F_5)_3$ and Et_3SiH in pentane under 10 bar of H_2 at ambient temperature. (6) In the absence of both H_2 and alkene, the reaction of **3a** with excess of $B(C_6F_5)_3$ and Me_2PhSiH in either benzene-d_6 or THF-d_8 afforded over 85% of **4a** and a small amount of **6a** (<10%), as well as an unknown species (<5%) showing a resonance at 34 ppm in the ^{31}P NMR spectrum. The η^2-H_2 ligand in **4a** must stem from the hydrolysis reaction between Me_2PhSiH and the aqua ligand of **3a**. (7) The FLP type phosphonium borate **6** proved to be inert toward catalysis, since hydrogenation of 1-hexene was not observed at 90 °C under 10 bar H_2 using 0.05 mol % of **6b**. All these results pointed to the formation of **6a**,**b** via intramolecular heterolytic cleavage of H_2 ligand by a neighboring phosphine ligand.[22]

dx.doi.org/10.1021/ja400135d | J. Am. Chem. Soc. 2013, 135, 4088−4102

2.3.2. Deuterium Isotope Studies. Deuterium isotope kinetics was pursued in the hydrogenation of 1-hexene at 23 °C under 10 bar of H_2 or D_2. In the case of "**3a**/Me_2PhSiH/$B(C_6F_5)_3$" and "**3a**/Et_3SiH/$B(C_6F_5)_3$" catalytic systems, inverse KIE values of 0.62 and 0.61 were determined, respectively. This suggested that the irreversible H−H splitting is not rate determining.[23] Under the catalytic condition applying D_2, the formed phosphonium borate was identified to be the deuterium derivative $[DP{i}Pr_3][HB(C_6F_5)_3]$ (100%) confirming a hydride transfer process from hydrosilane to $B(C_6F_5)_3$. The deuterium incorporation into the hexane starting from 1-hexene was examined via ^2H NMR revealing two singlets at 2.11 and 1.70 ppm. This confirmed the formation of 1,2-deuterated hexane expected for Wilkinson or Osborn type hydrogenations.[6c−e] The reaction thus went regio-specific. In the absence of H_2, 1-hexene could be isomerized with 10 mol % of **3a** and 50 mol % of "$Me_2PhSiH/B(C_6F_5)_3$" leading to (*Z*/*E*)-2-hexene in 30% conversion at 23 °C after 48 h. Apparently this alkene isomerization is comparatively slow and in no way competitive with the hydrogenation. A mechanism is suggested to involve a crucial hydride α-olefin rhenium complex, which via olefin insertion into a Re−H bond forms a secondary rhenium alkyl species. β-hydride elimination produces 2-hexene. The hydrogenation system was also found to be active in H_2/D_2 scrambling. When the mixture of **3a**, Me_2PhSiH and $B(C_6F_5)_3$ was treated in toluene with H_2/D_2 (550 mbar for each), the characteristic HD triplet signal at 4.50 ppm (J_{HD} = 44 Hz) was observed in the ^1H NMR spectra at 23 °C within 10 min.

2.3.3. VT-^{29}Si NMR Evidence for the Silylium Cation Induced Nitrosyl Activation. Variable temperature NMR experiments were carried out in order to further shed light on the possible intermediates. The ^{29}Si NMR spectrum of the mixture of Et_3SiH and $B(C_6F_5)_3$ in toluene-d_8 at −40 °C showed a new resonance at δ 9.8 ppm, which correlated with a triplet at 0.97 ppm and a quartet at 0.52 ppm in the ^1H NMR spectrum attributed to the formation of the H transferred intermediate possessing B−H···Si structures (Figure 5). Addition of 0.33 equiv of **4a** to the mixture at −40 °C revealed a new singlet at 30.3 ppm in the ^{29}Si NMR implying the coordination of a silyl cation to a Lewis basic atom.[24] The resonances of the ethyl group of the Re-NO-$SiEt_3$ moiety were observed as a triplet at 0.81 and a quartet at 0.63 ppm, as confirmed by ^{29}Si, ^1H correlation spectra. A Si−I bond, which is supposed to appear at ca. 8.6 ppm in ^{29}Si NMR spectrum, was not observed.[24] This again excluded that the activation course went via silylium induced iodo dissociation. The phosphonium borate **6a** was not formed at this stage as revealed by the absence of respective signals in both the ^1H and the ^{31}P NMR spectra. The trapped intermediate is unstable at low temperature and after warming to 23 °C it fully evolves into two species showing in the ^{29}Si NMR spectrum singlets at 29.2 and 34.8 ppm with complete consumption of Et_3SiH. In comparison, when **4a** was added to the mixture of $Et_3SiH/B(C_6F_5)_3$ at 23 °C, one more species was observed showing a singlet at 44.2 ppm in the ^{29}Si NMR spectrum. The ^{31}P NMR spectrum indicated the formation of **6a** along with three other new species at 60.2, 49.0, and 35.1 ppm. It was noticed that the singlet at 35.1 ppm was found to correlate with a triplet signal at 2.44 ppm (H_2, J = 26 Hz) and two multiplets at 2.49 and 1.19 ppm in the ^1H NMR spectrum. The downfield chemical shift of H_2 in comparison to that of **4** and the size of coupling constant of the triplet signal suggested the presence of a new dihydrogen complex possessing an electron-deficient Re center coordinated by two phosphine ligands.

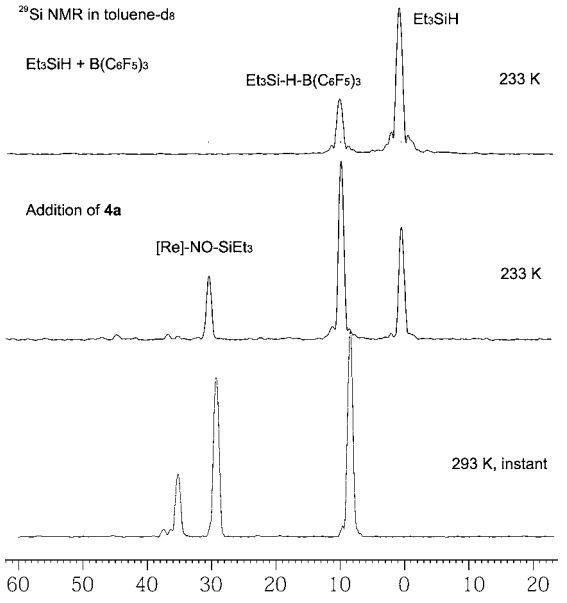

Figure 5. ^{29}Si NMR spectra recorded in toluene-d_8. (Top) Mixture of Et_3SiH and $B(C_6F_5)_3$ in 1:1 ratio at 233 K. (Middle) After addition of **4a** (in a ratio of 1:3 to Et_3SiH) into the mixture at 233 K within 10 s. (Bottom) After warming up to 293 K and immediate measurement.

2.3.4. ^{15}N NMR Evidence for the Silylium Cation Induced Nitrosyl Activation. ^{15}N NMR spectroscopy was utilized to provide further evidence for the nitrosyl activation pathway, in particular the facilitation of the nitrosyl bending.[25] A 98% ^{15}N-enriched rhenium diiodo dihydrogen complex $[ReI_2(^{15}NO)(PCy_3)_2(\eta^2\text{-}H_2)]$ (**4b-^{15}N**) was prepared starting from Re metal and ^{15}NO in a 7% overall yield using the synthetic method described in Scheme 2. The ^{15}NO gas was generated from $Na^{15}NO_2$ via the reaction with $FeSO_4$ and H_2O.[25] The ^{15}N NMR spectrum of **4b-^{15}N** was recorded in toluene-d_8 at 23 °C using CH_3NO_2 as external reference. It revealed a triplet at δ −49.4 ppm ($^2J_{N-P}$ = 5 Hz) due to coupling with the Re bound phosphorus ligand. When ca. 5 equiv. of $Me_2PhSiH/B(C_6F_5)_3$ (1:1) were added to the toluene solution of **4b-^{15}N**, the triplet signal immediately disappeared concomitant with the appearance of two new resonances observed as a doublet at δ 105.9 ppm ($^2J_{N-P}$ = 5 Hz) and a singlet at δ 90.8 ppm corresponding to a monophosphine and a phosphine-free species, respectively. The large downfield chemical shift in the ^{15}N NMR upon addition of the cocatalytic system would be in accord with the reported observation of chemical shift changes when linear nitrosyls transform into bent ones.[26] Together with the ^{29}Si NMR spectroscopic observations, this is interpreted in terms of attachment of the silylium cation to the O_{NO} atom supporting the NO bending.

2.3.5. DFT Investigation of Silylium Facilitated NO Bending. Four model systems **I**, **II**, **I-SiMe$_3$** and **II-SiMe$_3$** (**-1** and **-2**) derived from the complex $[ReI_2(NO)(PMe_3)_2(\eta^2\text{-}H_2)]$ bearing either *trans*- or *cis*-diiodide ligands with or without $SiMe_3^+$ Lewis acid attached, were investigated in more detail by DFT calculations. Their geometries were optimized at TPSS level[12] employing the large Gaussian AO-basis set def2-TZVP[13] and the D3 dispersion correction.[14] Subsequent single-point calculations with the double-hybrid functional B2PLYP-D3[15] and the same basis set were carried out to yield the energy

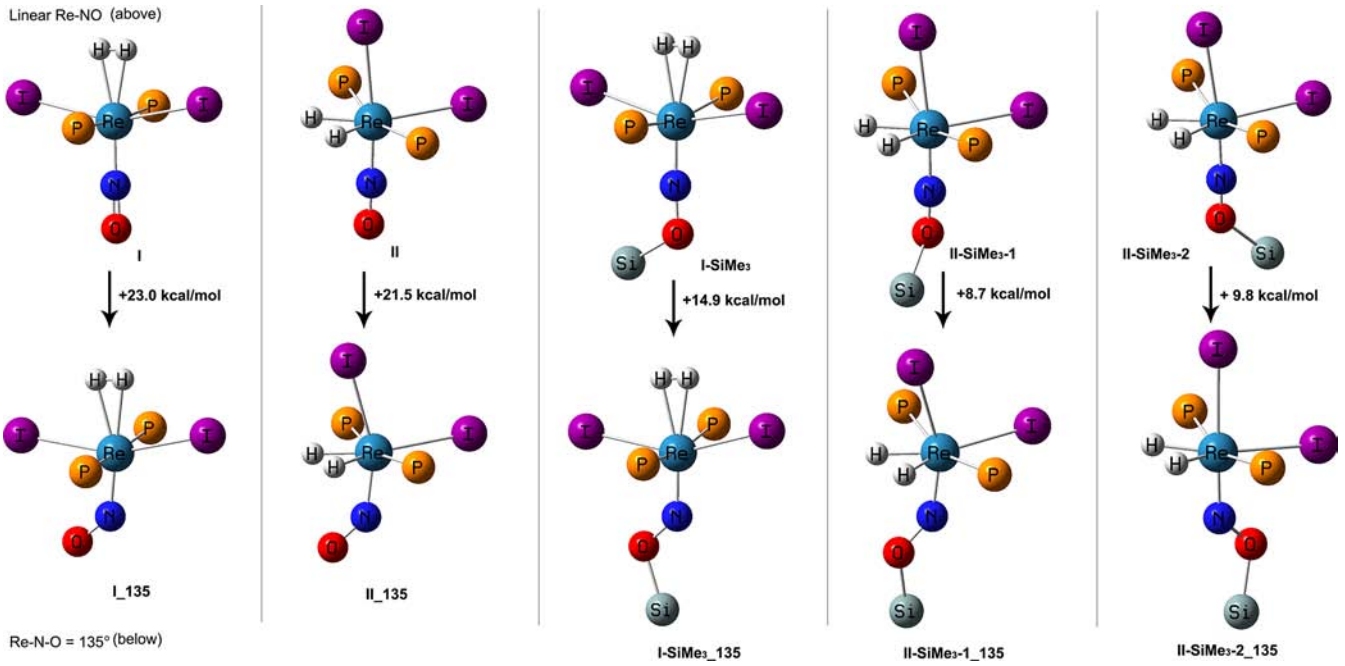

Figure 6. Sketches of local energy minimum structures of five rhenium dihydrogen diiodide systems (with linear and bent nitrosyl ligands Re−N−O = 135°). **I**: H−H eclipses I−Re−I axis. **II**: H−H eclipses P−Re−P axis. **I-SiMe$_3$**: H−H eclipses I−Re−I axis with Si atom on O_{NO}. **II-SiMe$_3$-1**: H−H eclipses P−Re−P axis with Si atom orientated *cisoid* to H_2. **II-SiMe$_3$-2**: H−H eclipses P−Re−P axis with the Si atom orientated *transoid* to H_2. All the carbon and hydrogen atoms except for the H_2 ligand are omitted for clarity.

Table 2. Relative Energies and Geometry Parameters of the Local Minima Obtained upon the Bending of Nitrosyl Ligand

	I		**II**		**I-SiMe$_3$**		**II-SiMe$_3$-1**			**II-SiMe$_3$-2**		
Re−N−O (°)	180.0	135.0	178.1	135.0	175.5	134.5	180.0	135.0	120.5	176.6	135.0	120.0
Δ*E* (kcal/mol)	0.0	+23.0	0.0	+21.5	0.0	+14.9	0.0	+8.7	+20.4	0.0	+9.8	26.5
I1−Re−N (deg)	101.7	90.2	173.4	156.9	102.5	96.3	168.8	155.8	152.5	174.0	176.9	178.0
I2−Re−N (deg)	101.2	110.3	92.1	102.0	102.5	109.0	96.8	102.3	99.5	91.0	84.5	86.6
Re−N (Å)	1.767	1.788	1.777	1.806	1.728	1.763	1.748	1.777	1.777	1.737	1.787	1.787
N−O (Å)	1.185	1.232	1.183	1.227	1.287	1.339	1.269	1.311	1.311	1.153	1.306	1.307
H−H (Å)	0.790	0.785	1.527	1.494	0.787	0.783	1.560	1.512	1.525	1.512	1.533	1.483
Re−H1 (Å)	2.008	2.078	1.662	1.657	2.075	2.076	1.660	1.656	1.655	1.662	1.668	1.670
Re−H2 (Å)	2.006	2.097	1.662	1.657	2.076	2.114	1.660	1.657	1.656	1.662	1.671	1.673

values discussed below. These values possess an estimated accuracy of about 1 −2 kcal/mol. All calculated structures are calculated to be local energy minima. Selected examples with linear NO and bent NO at 135° are displayed in Figure 6. The geometric parameters obtained from the molecules with NO bending are listed in Table 2. For the type **I** and **II** complexes, relative energies of 23.0 and 21.5 kcal/mol, respectively, were calculated for the bending of the Re−N−O angle to 135°, demonstrating that both conformers prefer a linear NO arrangement and that a considerable energetic demand would be necessary to achieve even small bending angles. The type **I** complex with the H−H axis eclipsing the I−Re−I axis shows a lower preference for the NO bending than the type **II** complex with H−H eclipsing the P−Re−P axis. In both cases, the iodide ligand *cis* to the nitrogen atom is slightly bent away from the NO ligand and the I2−Re−N angle increases along with bending of the NO ligand. At the same time, the Re−N and N−O bond distances increase with the bending of the Re−N−O angle. The enhanced π-back-donation from the Re center to NO leads to decreased bond orders.

Upon attachment of the $SiMe_3^+$ Lewis acid to the nitrosyl ligand, NO bending was facilitated in the **I-SiMe$_3$** and **II-SiMe$_3$** complexes. For instance, a smaller energy of 14.9 kcal/mol was required to achieve a bending angle of 135° for **I-SiMe$_3$** in comparison to 23.0 kcal/mol for **I**. Further bending to 130° resulted in full dissociation of the dihydrogen ligand *trans* to the bent NO group. In the case of **II-SiMe$_3$**, two isomers are present: **II-SiMe$_3$-1** with coordinated silylium *cisoid* to the dihydrogen ligand and **II-SiMe$_3$-2** with coordinated silylium *transoid* to the dihydrogen ligand. Comparing the two conformers with linear Re−N−O angles, the **II-SiMe$_3$-1** is found to be 7.8 kcal/mol more stable than **II-SiMe$_3$-2**. Such an orientational preference of the silylium residue can only be interpreted in one way - steric repulsion between the H_2 and $SiMe_3^+$ units is much smaller than between the iodo and $SiMe_3^+$ moieties. It is worth mentioning that the large energy difference between **I** and **II** (18 kcal/mol) decreased to 9.6 kcal/mol between **I-SiMe$_3$** and **II-SiMe$_3$-2**. This can be explained by the fact that the *trans* influence of the nitrosyl ligand, which is the main cause for the instability of **I**, is weakened by coordination of the silylium ion to the O_{NO} atom. That way the effect that the Lewis acid facilitates NO bending is more pronounced in the case of **II-SiMe$_3$** (**-1** and **-2**). The energies for bending the Re−N−O angle to 135° are rather small with only 8.7 kcal/mol

dx.doi.org/10.1021/ja400135d | *J. Am. Chem. Soc.* 2013, 135, 4088−4102

Scheme 5. Proposed Nitrosyl Activation Pathway and an Osborn-type Catalytic Cycle

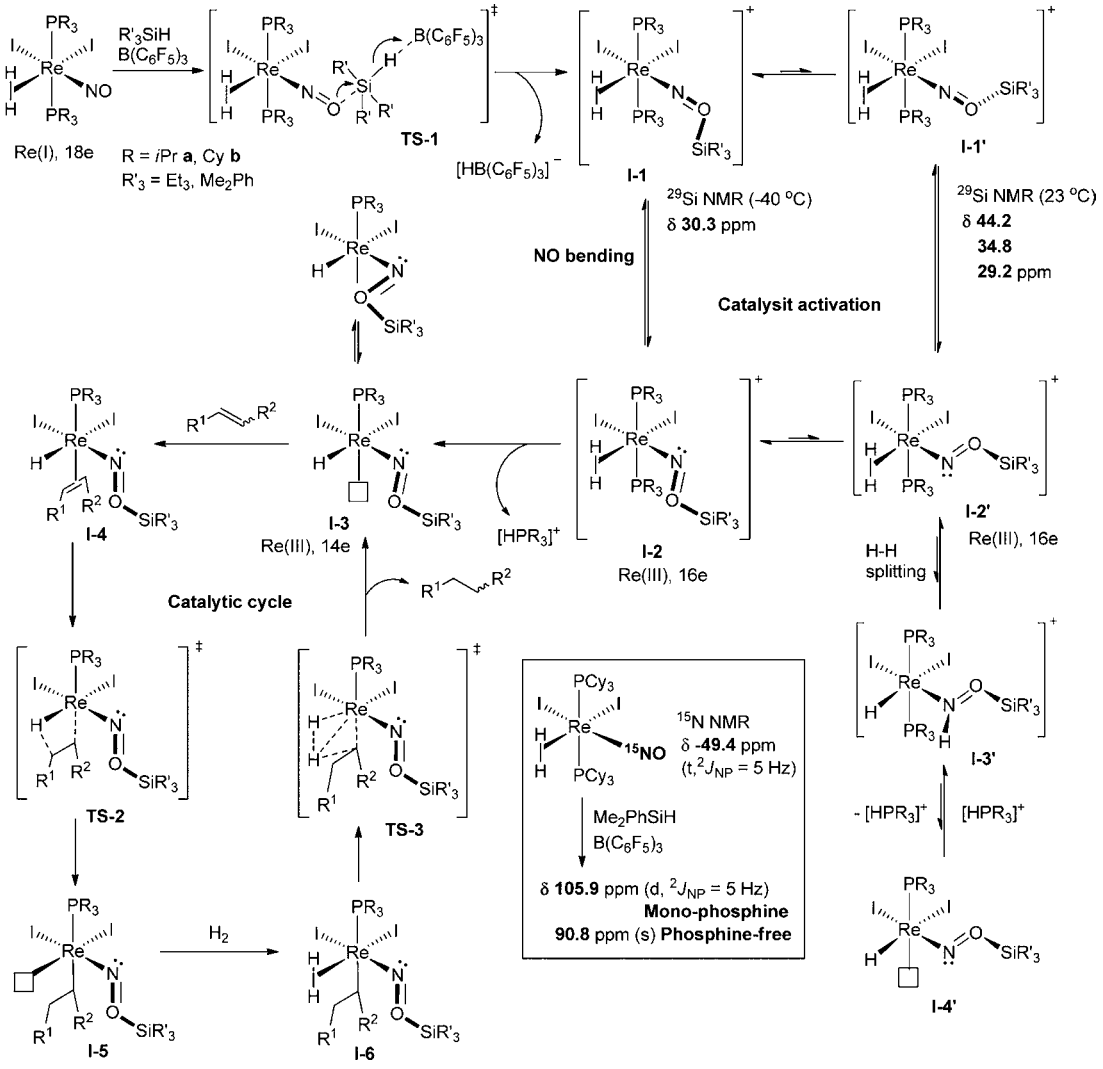

for **II-SiMe$_3$-1** and 9.8 kcal/mol for **II-SiMe$_3$-2**. The angle between the two iodide ligands in **II-SiMe$_3$-1** widens up to 102.3°, which emphasizes the additional potential for coordination of a ligand. At 135° **II-SiMe$_3$-1** could be calculated to be 8.9 kcal/mol more stable than **II-SiMe$_3$-2**. The lone pair of the N_{NO} atom on the bent nitrosyl moiety of **II-SiMe$_3$-1** repels the neighboring iodo ligand resulting in a N−Re−I2 angle of 101.9° and N−Re−I1 angle of 155.7°. Compared to this, repulsion of the dihydrogen ligand by the lone pair of the N_{NO} atom in the bent **II-SiMe$_3$-2** is less effective showing a reduced N−Re−I2 angle of 84.5°. Further bending of the Re−N−O angle to 120.5° in **II-SiMe$_3$-1** requires 20.4 kcal/mol relative to the linear nitrosyl case. Similarly, the bond orders of the Re−N and N−O bonds decrease along with the extent of NO bending.

2.3.6. Proposed Activation Pathway and Catalytic Cycle. The activation pathway of the rhenium catalysts by the "hydrosilane/B$(C_6F_5)_3$" co-catalytic systems is expected to go along with the generation of phosphonium borate, as depicted in Scheme 5. It is most likely that in the initiation stage reversible coordination of the B$(C_6F_5)_3$ Lewis acid to the Si−H bond of the hydrosilane occurs affording an intermediate bearing hyperconjugative B···H−Si and B−H···Si resonance structures.[10,11]

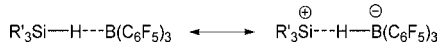

This activates the silicon group for R′$_3$Si$^+$ transfer to the Lewis basic nitrosyl oxygen atom of **4** via the **TS-1** transition state accompanied by full hydride transfer from the hydrosilane to B$(C_6F_5)_3$. As verified by the DFT calculations, intermediate **I-1** with the Si atom oriented toward the H_2 is favored over its isomer **I-1′** with the Si atom oriented toward the iodo ligand. Subsequently, nitrosyl bending occurs affording the 16e$^-$ Re(III) species **I-2**, in which the lone pair electron of the bent nitrosyl moiety is *anti* to the H_2 ligand. A vacant site is expected to be generated forming a seven-coordinate Re(III) species. However, this is apparently prevented by the *cis*-labilizing effect of the two iodides in **I-2** promoting the six-coordinate geometry. In **I-2**, the Re center is more electron-deficient turning the η^2-H_2 ligand acidic, or in other words, highly polarized toward $H^{\delta+}$-$H^{\delta-}$.[16,27] The crypto-H$^+$ is readily transferred to the neighboring in-plane *cis*-phosphorus atom affording the hydride **I-3** accompanied by formation of the phosphonium borate **6**.[22]

The "superelectrophilic" 14e$^-$, Re(III) hydride species **I-3** serves as the basic catalytic intermediate driving the hydrogenation cycle along an Osborn-type scheme with alkene before H_2 addition.[6d,e] Importantly, the vacant site in **I-3** can open up

dx.doi.org/10.1021/ja400135d | J. Am. Chem. Soc. 2013, 135, 4088−4102

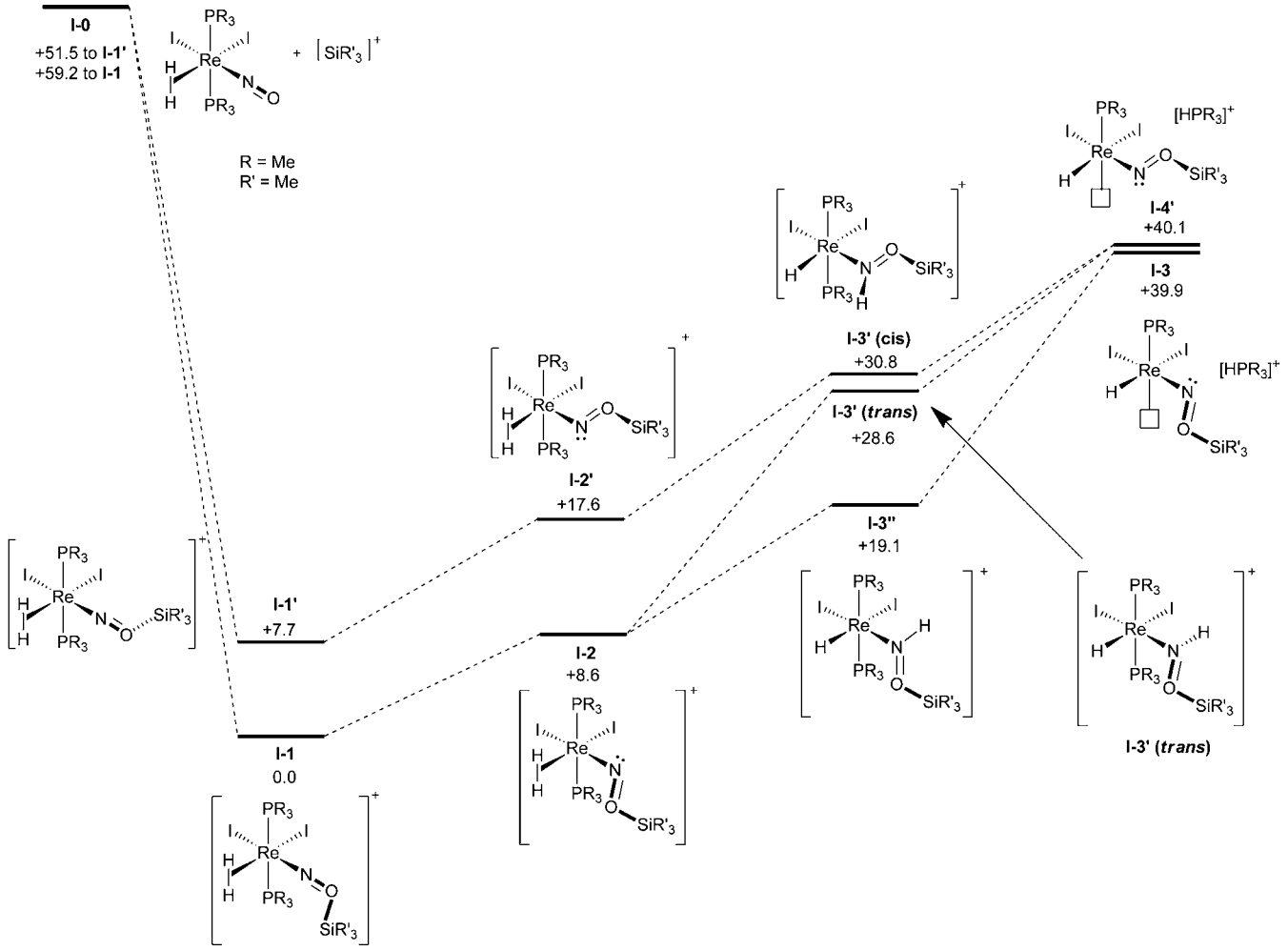

Figure 7. B2PLYP-D3/def2-TZVP calculated ΔE (kcal/mol) of the structurally optimized model complexes along the catalyst activation course.

on-demand, eventually stabilized by interaction with the lone pair of the O_{NO} atom. This neighboring group effect provides protection to the unsaturated species and might account for the longevity of the catalyst. It should also be emphasized here that although the pK_a value of the bound H_2 in the intermediate **I-2** cannot be determined due to its high instability, the phosphine ligand is considered to be basic enough (for instance with a pK_a(aq) of 9.70 for PCy_3)[28] to abstract a proton from the polarized H−H ligand supposedly in the transition state of its elimination. The basicity of $PiPr_3$ is slightly weaker than that of PCy_3, but still in the range that the deprotonation can happen. This higher basicity of PCy_3 might account for the higher activity of the catalytic system with **3b** due to a more efficient intramolecular heterolytic H_2 cleavage and faster phosphine liberation producing higher concentrations of the **I-3** type species.

Parallel to this, another pathway is proposed based on the thermodynamically less favored isomer **I-2′**, which can be derived from either nitrosyl bending of **I-1′** or isomerization of **I-2**. The fact that several singlets in a close chemical shift range evolved in the ^{29}Si NMR spectra of stoichiometric reactions with the $Et_3SiH/B(C_6F_5)_3$ reagent (Figure 4) supports the idea that structurally related species exist which all bear Re-NO-Si moieties. **I-2′** is quite interesting due to the *cis*-alignment of the H_2 ligand and the lone pair of the N_{NO} atom available by bending. In a similar fashion to the Noyori-Morris type catalysts,[29] H−H heterolytic cleavage of the polarized H_2 ligand across the Re−N bond could occur affording the intermediate **I-3′**. This step would demonstrate a novel cooperative function of the bent nitrosyl ligand especially suited for H_2 catalyzes with polar reactivity characteristics.[30] The N−H moiety in **I-3′** is then thought to be deprotonated by a labile *cis*-positioned phosphine ligand affording the 14e$^-$ Re(III) hydride **I-4′**, which is an isomer of **I-3**, but more activated due to the lack of stabilization. **I-4′** can enter the Osborn-type hydrogenation cycle, or eventually isomerize to **I-3**.

2.3.7. DFT Calculations in Support of the Catalyst Activation Path. To support the proposed activation pathways, dispersion corrected DFT (B2PLYP-D3/def2-TZVP//TPSS-D3/def2-TZVP) calculations were carried out. The free energy profiles connecting the most plausible species are depicted in Figure 7. Coordination of the $SiMe_3^+$ moiety to the O_{NO} atom of the model PMe_3 complex is highly exothermic with an energy of −51.5 and −59.2 kcal/mol forming **I-1**(PMe_3) and **I-1′**(PMe_3), respectively (reactants are included as structure **I-0** in Figure 7). A bending angle of 135° of the Re−N−O unit leads to **I-2**(PMe_3) and **I-2′**(PMe_3) positioned at somewhat elevated energies of 8.7 and 9.8 kcal/mol relative to **I-1**(PMe_3) and **I-1′**(PMe_3), respectively. Heterolytic cleavage of the H−H bond by the basic nitrogen atom of **I-2**(PMe_3) would require an additional energy of 13.2 kcal/mol to form **I-3′**(PMe_3)(*cis*) bearing *syn*-positioned Re−H and N−H bonds at an energy of

dx.doi.org/10.1021/ja400135d | J. Am. Chem. Soc. 2013, 135, 4088−4102

30.8 kcal/mol relative to the reference conformer. The formation of the alternative isomer possessing *trans*-Re−H and N−H bonds is at a slightly lower energy of 28.6 kcal/mol. The H−H bond cleavage in **I-2**(PMe_3) leads to another isomer bearing *anti*-Re−H and N−H bonds at an energy of 10.4 kcal/mol. However, the transition state for the H−H splitting process could not be located. The deprotonation of the N−H bond by a phosphine ligand demands an energy of 9.3 kcal/mol starting from **I-3′**(PMe_3)(*cis*). Alternatively, the energy of the monophosphine isomer **I-3**(PMe_3) with the lone pair on the N_{NO} atom *trans* to the Re−H was calculated to be 39.9 kcal/mol relative to the start conformer. Since this reaction course is highly endothermic, it is kinetically not very probable. Coordination of either olefin or H_2 to **I-4′**(PMe_3) or **I-3**(PMe_3) drastically decreases the energy of the newly formed species, and would therefore render the overall hydrogenation reaction thermodynamically feasible. The high energy level of the 14e$^-$ hydride **I-4′**(PMe_3) or **1-3**(PMe_3) with bent NO ligands also implies that the 16e$^-$ hydride isomers bearing a linear NO ligand[2c,d] might also be involved in the catalytic cycle.

*2.3.8. Exclusion of the Formation of an Initial Iodo Hydride Complex from **4a,b** and the Hydrosilane.* In an earlier publication, we discovered the pentacoordinate bromo complex of the type [ReBr(H)(NO)(PR_3)$_2$] to show high activities in the hydrogenation of olefins when boron Lewis acids were applied as sole co-catalysts.[8] In contrast to the bromo case where the bromo hydride could quantitatively be obtained from the dibromo precursor, the analogous reaction of the [ReI_2(NO)(PCy_3)$_2$(η^2-H_2)] (**4b**) with Et_3SiH at 100 °C afforded only a complex mixture and a large amount of unreacted **4b**. The much lower tendency of the iodo complex to react with hydrosilanes might be attributed to the fact that the Si−I bond (about 56 kcal/mol) is of much lower thermodynamic strength than the Si−H bond (about 76 kcal/mol), while the Si−Br bond (74 kcal/mol) is close in energy to the Si−H bond.[31] Nevertheless, in order to exclude the pathway involving initial formation of an iodo hydride complex from **3** and Et_3SiH followed by $B(C_6F_5)_3$ activation, the five coordinate iodo hydride **8b** was exemplarily prepared by a route as depicted in Scheme 6. Starting from [$ReBr_2$(H)(NO)(PCy_3)$_2$],[32] halide exchange with NaI in THF afforded at 23 °C within 15 h the Re(II) iodo hydride [ReI_2(H)(NO)(PCy_3)$_2$] (**7b**) in 82% yield. The IR spectra showed a strong ν(Re−H) absorption at 2006 cm^{-1} and a ν(NO) absorption at 1684 cm^{-1}. The molecular structure of **7b** was established by a X-ray diffraction study, as depicted in Figure 8. Similar to the bromo derivative, **7b** adopted a pseudo-octahedral geometry around the rhenium center. The two *trans*-phosphine ligands are bending over strongly toward the hydride ligand with a P1−Re1−P2 angle of 148.40(2)°.

Scheme 6. Synthesis of the Re(I) Iodo Hydride 8b

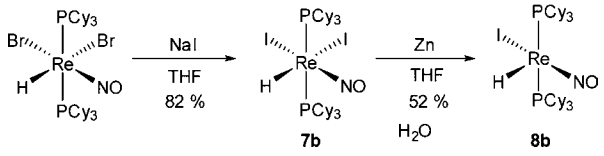

Reduction of **7b** with Zn in THF at 23 °C for 15 h afforded a deep purple solution, from which the five-coordinate Re(I) iodo hydride complex [ReI(H)(NO)(PCy_3)$_2$] (**8b**) could be isolated in 52% yield by extraction with pentane. The IR spectrum showed a strong ν(NO) absorption at 1657 cm^{-1}. The ^{1}H NMR spectrum in benzene-d_6 exhibited a broad unresolved triplet at δ −15.9 ppm for the hydride ligand. The ^{31}P{^{1}H}-NMR spectrum displayed a singlet at δ 31.2 ppm. Finally, the catalytic performance of **8b** in the hydrogenation of 1-hexene was tested in the presence of $B(C_6F_5)_3$. At 23 °C under 10 bar of H_2, a TON of 1830 was obtained within 30 min corresponding to a conversion of 18% and a TOF of 3661 h^{-1}, which is by far not comparable to those TOFs obtained with the "**3b**/Et_3SiH/$B(C_6F_5)_3$" system. On the basis of these experiments, we excluded the formation of iodo hydride complexes of type **8b** in the course of the activation process of the "**3b**/Et_3SiH/$B(C_6F_5)_3$" catalytic system.

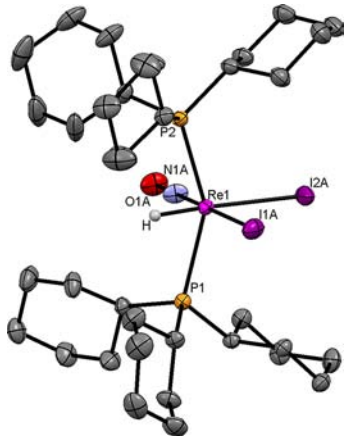

Figure 8. Molecular structure of [ReI_2(H)(NO)(PCy_3)$_2$] (**7b**) with 50% probability displacement ellipsoids. Hydrogen atoms have been omitted for clarity. Selected bond lengths (Å) and angles (deg): I(1A)-Re(1), 2.7520(2); I(2A)-Re(1), 2.7498(3); P(1)−Re(1), 2.4794(6); P(2)−Re(1), 2.4865(6); N(1A)-O(1A), 1.195(3); P(1)−Re(1)−P(2), 148.40(2); P(1)−Re(1)−I(2A), 105.825(15); P(2)−Re(1)−I(2A), 105.770(16); P(1)−Re(1)−H, 73.4(12); P(2)−Re(1)−H, 75.1(12).

3. CONCLUSIONS

In this article, the first example of a "catalytic nitrosyl effect" with activation by NO bending was demonstrated. This bending generated an open site, which contributed to the reaction course of highly efficient hydrogenation catalyzes. The "Re(I) diiodide/hydrosilane/$B(C_6F_5)_3$" co-catalytic systems could be tuned to eventually furnish the most efficient rhenium catalyst so far known for the hydrogenation of alkenes. Both the activity and longevity are superior to previously reported catalytic systems. The remarkable catalytic performance is boosted by the bending of the ReNOSi moiety assisted by the *in situ* attached silylium ions followed by intramolecular heterolytic dihydrogen cleavage in the catalyst's activation course. The coordination of a Lewis acid to NO is vital to accomplish excellent catalytic performance. DFT calculations could show this mechanism to be plausible and proof the importance of the silyl-coordination for the reactions course. This work demonstrates ways of utilization of middle transition metals via a tuning of ligand effects to replace platinum group metals in highly efficient catalytic applications. A new protocol and strategy to improve the catalytic performance of nitrosyl transition metal complexes could be established. Further exploration and exploitation in catalysis of the Lewis acid induced nitrosyl bending, denoted as the "catalytic nitrosyl effect", is currently under investigation in our group.

4. EXPERIMENTAL SECTION

4.1. General Experimental. All manipulations were carried out under an atmosphere of dry nitrogen using standard Schlenk techniques or in a glovebox (M. Braun 150B-G-II) filled with dry nitrogen. Solvents were freshly distilled under N_2 by employing standard procedures and were degassed by freeze−thaw cycles prior to use. The deuterated solvents were dried with sodium/benzophenone (toluene-d_8, benzene-d_6, THF-d_8) or P_2O_5 (chlorobenzene-d_5) and hvacuum transferred for storage in Schlenk flasks fitted with Teflon valves. ^{1}H NMR, ^{13}C{^{1}H}-NMR, ^{31}P{^{1}H}-NMR, ^{19}F NMR and ^{11}B NMR data were recorded on a Varian Gemini-300, Varian Mercury 200, or Bruker DRX 500 spectrometers using 5 mm diameter NMR tubes equipped with Teflon valves, which allow degassing and further introduction of gases into the probe. Chemical shifts are expressed in parts per million (ppm). ^{1}H and ^{13}C{^{1}H}-NMR spectra were referenced to the residual proton or ^{13}C resonances of the deuterated solvent. All chemical shifts for the ^{31}P{^{1}H}-NMR data are reported downfield in ppm relative to external 85% H_3PO_4 at 0.0 ppm. Signal patterns are reported as follows: s, singlet; d, doublet; t, triplet; m, multiplet. IR spectra were obtained by using KBr pellets or ATR methods with a Bio-Rad FTS-45 FTIR spectrometer. Microanalyses were carried out at the Anorganisch-Chemisches Institut of the University of Zurich. Complexes **1** were prepared according to reported procedures.[4b] $B(C_6F_5)_3$, $Na^{15}NO_2$, AlF_3 and diverse alkenes were purchased from Aldrich and used without further purification. 1-Hexene, 1-octene, cyclooctene, and 1,5-cyclooctadiene were purified by distillation.

4.2. General Procedure for Hydrogenation of Alkenes Catalyzed by the "[Re]/Hydrosilane/B(C_6F_5)$_3$" System. In a 30 mL steel autoclave equipped with a stirring bar, certain amounts of the substrate alkene (e.g., 1-hexene, 2.5 mL, 20 mmol; 1-octene, 2.5 mL, 16 mmol; cyclooctene, 1 mL, 8 mmol; 1,5-cyclooctadiene, 1 mL, 8 mmol; cyclohexene, 2 mL, 20 mmol; styrene, 1 mL, 9 mmol; 1,7-octadiene, 1 mL, 7 mmol), appropriate amount of rhenium catalyst (**3a**, 1.5 mg, 0.002 mmol; **3b**, 2.0 mg, 0.002 mmol; **4a**, 1.6 mg, 0.002 mmol; **4b**, 2.1 mg, 0.002 mmol; **7a**, 1.1 mg, 0.002 mmol; **7b**, 1.6 mg, 0.002 mmol), 5 equiv of $B(C_6F_5)_3$ (5.2 mg, 0.01 mmol) and 5 equiv of hydrosilane (Et_3SiH, 1.6 μL, 0.01 mmol; Me_2PhSiH, 1.6 μL, 0.01 mmol; $MePh_2SiH$, 2.0 μL, 0.01 mmol; iPr_3SiH, 2.0 μL, 0.01 mmol; Ph_3SiH, 2.6 mg, 0.01 mmol) were mixed. After being flushed with 3.7 bar of H_2 thrice, the system was charged with 10 bar of H_2 and kept stirring at either ambient temperature or 90 °C. The progress of the reactions was monitored by a Buechi Pressflow Gas Controller and the conversion of the hydrogenations was calculated based on the consumption of H_2 in the system. When 40 bar of H_2 was employed, the reaction course was monitored by the decreased pressure of autoclave. The hydrogenation products were characterized by ^{1}H NMR spectroscopy in $CDCl_3$. The TONs and TOFs values were determined based on the consumption of H_2.

*4.2.1. [$ReBr_2(NO)(PiPr_3)_2(H_2O)$] (**2a**).* In a 3 mL Young-NMR-Tube, **1a** (70 mg, 0.10 mmol) was mixed with degassed H_2O (90 μL) and THF (0.5 mL). The solution was kept at 90 °C for 5 min resulting in the formation of an orange solution. ^{31}P NMR spectra indicated the full conversion of the starting material. The reaction mixture was cooled to room temperature and filtered through Celite. The solvent was evaporated and the residue was further washed with pentane (2 × 2 mL), dried *in vacuo* giving an orange solid: 69 mg; yield, 96%. **2a:** IR (KBr, cm^{-1}): ν(O−H) 3428 (br), ν(C−H) 2963, 2924, 2873, 1460, ν(NO) 1667. ^{1}H NMR (300.08 MHz, THF-d_8, ppm): δ 5.72 (s, 2H, H_2O), 3.06 (m, 6H, PCH(CH_3)$_2$), 1.32−1.38 (m, 36H, PCH(CH_3)$_2$). ^{13}C{^{1}H}-NMR (75.47 MHz, THF-d_8, ppm): δ 25.6 (t, $J_{(PC)}$ = 10 Hz, P-CH), 20.0 (s, PCH(CH_3)$_2$). ^{31}P{^{1}H}-NMR (121.47 MHz, THF-d_8, ppm): δ −5.9. ^{1}H NMR (300.08 MHz, benzene-d_6, ppm): δ 4.90 (broad, 2H, H_2O), 3.07 (m, 6H, PCH(CH_3)$_2$), 1.26−1.36 (m, 36H, PCH(CH_3)$_2$). ^{13}C{^{1}H}-NMR (75.47 MHz, benzene-d_6, ppm): δ 25.1 (t, $J_{(PC)}$ = 10 Hz, P-CH), 20.0 (s, PCH(CH_3)$_2$). ^{31}P{^{1}H}-NMR (121.47 MHz, benzene-d_6, ppm): δ −4.7. Anal. Calcd for $C_{18}H_{44}Br_2NO_2P_2Re$ (713,08): C, 30.26; H, 6.21; N, 1.96. Found: C, 30.60; H, 6.11; N, 1.72.

*4.2.2. [$ReI_2(NO)(PiPr_3)_2(H_2O)$] (**3a**).* In a 20 mL vial in glovebox, **2a** (36 mg, 0.05 mmol) and excess of NaI (105 mg, 0.7 mmol) were mixed in 3 mL of THF. A yellow-brown solution immediately formed, and after stirring at room temperature for 2 h, a unique organometallic species is present in solution as indicated by ^{31}P NMR spectra. The mixture was filtered through a glass sintered funnel and the filtrate was dried *in vacuo*. The residue was extracted with benzene (2 × 2 mL) and dried *in vacuo*. The obtained brown solid was washed again with pentane (2 × 2 mL), dried *in vacuo* giving a brown solid. Yield: 38 mg, 0.047 mmol, 94%. IR (KBr, cm^{-1}): ν(O−H) 3435 (br), ν(C−H) 2961, 2926, 2871, 1458, ν(NO) 1674. ^{1}H NMR (300.08 MHz, THF-d_8, ppm): δ 5.43 (s, 2H, H_2O), 3.40 (m, 6H, PCH(CH_3)$_2$), 1.33−1.43 (m, 36H, PCH(CH_3)$_2$). ^{13}C{^{1}H}-NMR (75.47 MHz, THF-d_8, ppm): δ 27.5 (t, $J_{(PC)}$ = 10 Hz, P-CH), 20.3 (s, PCH(CH_3)$_2$). ^{31}P{^{1}H}-NMR (121.47 MHz, THF-d_8, ppm): δ −10.7. Anal. Calcd for $C_{18}H_{44}I_2NO_2P_2Re$ (809,05): C, 26.74; H, 5.49; N, 1.73. Found: C, 26.87; H, 5.36; N, 1.65.

*4.2.3. [$ReI_2(NO)(PCy_3)_2(H_2O)$] (**3b**).* **Method 1:** In a 100 mL round-bottom flask, H_2O_2 (5 mL, 30%) was added dropwise to Re powder (1.5 g, 8.0 mmol) at 0 °C. NEt_4I (2.5 g, 9.5 mmol) was then added and the mixture was stirred for 3 h at 90 °C. After that, additional part of NEt_4I (2.5 g, 9.5 mmol) was added, and the mixture was dissolved in 30 mL of HI (57%) and 3 mL of H_3PO_2 (50%). NO gas was bubbled through the solution at 110 °C. Twenty hours later, the reaction mixture was cooled down to room temperature and was filtered. The collected dark residue was extracted with MeOH (10 × 5 mL) and the solvent was evaporated *in vacuo*. The obtained residue was further washed with H_2O (5 × 10 mL) and diethyl ether (5 × 10 mL), dried *in vacuo* affording a dark blue solid. Yield: 1.8 g. A mixture of this crude compound (180 mg) and PCy_3 (170 mg, 0.61 mmol) suspended in ethanol (5 mL) was stirred at 90 °C for 15 h. During this reaction time, a brown precipitate gradually formed. The reaction mixture was cooled to room temperature and filtered. The residue was washed with ethanol (2 × 2 mL) and dried *in vacuo* giving a brown solid. Yield: 183 mg, 20% (overall). IR (ATR, cm^{-1}): ν(O−H) 3566 (br), ν(C−H) 2916, 2848, 1444, ν(NO) 1644. ^{1}H NMR (300.08 MHz, THF-d_8, ppm): δ 5.20 (s, 2H, H_2O), 3.16 (br, 6H, P-CH), 1.24−2.13 (m, 60H, CH_2). ^{13}C{^{1}H}-NMR (75.47 MHz, THF-d_8, ppm): δ 36.3, 29.1, 27.8, 26.7. ^{31}P{^{1}H}-NMR (121.47 MHz, THF-d_8, ppm): δ −19.1. Anal. Calcd for $C_{36}H_{68}I_2NO_2P_2Re$ (1048,89): C, 41.22; H, 6.53; N, 1.34. Found: C, 41.09; H, 6.70; N, 1.39. **Method 2:** $[NEt_4]_2[ReBr_5(NO)]$ (1.0 g, 1.14 mmol) was treated with excess of NaI (10.0 g, 7.33 mmol) in 20 mL of THF. The mixture was kept stirring at 90 °C for 24 h. The resultant deep blue solution was filtered through a glass sintered funnel to remove NaBr. The collected solution was dried *in vacuo*, and further washed with H_2O (3 × 5 mL) to afford a crude Re(II) iodonitrosyl product. Single-crystals were formed from layered solutions of THF and diethyl ether, and were shown by X-ray diffraction studies to be the $[NEt_4][ReI_4(NO)(THF)]$ complex. IR (ATR, cm^{-1}): ν(C−H) 2969, 2921, 2852, ν(NO) 1734. Anal. Calcd for $C_{12}H_{28}I_4N_2O_2Re$ (926.19): C, 15.56; H, 3.05; N, 3.02. Found: C, 15.29; H, 3.10; N, 3.15. As a matter of fact, purification of the crude product is not necessary as the impurity could be removed in the subsequent step. The reaction of the crude Re(II) compound (500 mg) with PCy_3 (650 mg, 2.32 mmol) in 10 mL of ethanol and 10 drops of H_2O afforded at 90 °C within 15 h a brown precipitate, which was isolated and washed with ethanol (4 × 5 mL) affording the compound **3b**. Yield: 351 mg, 67% (overall).

*4.2.4. [$ReI_2(NO)(PR_3)_2(\eta^2\text{-}H_2)$] (**4**, R = iPr a, Cy b).* In a 50 mL Young-Schlenk tube, **3a** (34 mg, 0.04 mmol) or **3b** (54 mg, 0.05 mmol) was mixed with excess of anhydrous $MgSO_4$ in 3 mL of benzene. The N_2 atmosphere was replaced with 1.3 bar of H_2 by using a freeze−pump−thaw cycle. After warming up to room temperature, NMR spectroscopy indicated the instantaneous formation of the hydrogen coordinated rhenium diiodo complex **4a** or **4b** in 100% *in situ* yield. The reaction was kept at room temperature for overnight, the mixture was filtered through a glass sintered funnel and the filtrate was dried *in vacuo*. **4a:** 25 mg. Yield: 74%. IR (ATR, cm^{-1}): ν(C−H) 2960, 2922, 2873, 1456, ν(NO) 1719. ^{1}H NMR (300.08 MHz, benzene-d_6, ppm): δ 3.06 (m, 6H, PCH(CH_3)$_2$), 1.28−1.39 (m, 18H,

dx.doi.org/10.1021/ja400135d | J. Am. Chem. Soc. 2013, 135, 4088−4102

PCH(CH_3)$_2$), 1.06−1.16 (m, 18H, PCH(CH_3)$_2$), 0.89 (t, $^2J_{(HP)}$ = 22 Hz, 2H, H_2). ^{1}H NMR (300.08 MHz, THF-d_8, ppm): δ 3.18 (m, 6H, PCH(CH_3)$_2$), 1.34−1.43 (m, 36H, PCH(CH_3)$_2$), 0.64 (t, $^2J_{(HP)}$ = 20 Hz, 2H, H_2). ^{13}C{^{1}H}-NMR (75.47 MHz, benzene-d_6, ppm): δ 26.1 (t, $J_{(PC)}$ = 11 Hz., P-CH), 20.5 (s, PCH(CH_3)$_2$), 19.8 (s, PCH(CH_3)$_2$). ^{31}P{^{1}H}-NMR (121.47 MHz, benzene-d_6, ppm): δ 3.09. Anal. Calcd for $C_{18}H_{44}I_2NOP_2Re$ (792.51): C, 27.28; H, 5.60; N, 1.77. Found: C, 26.99; H, 5.51; N, 1.72. **4b:** 39 mg, 76%. IR (ATR, cm^{-1}): ν(C−H) 2926, 2850, 1445, ν(NO) 1710. ^{1}H NMR (300.08 MHz, benzene-d_6, ppm): δ 1.10−3.00 (m, 68H, P(C_6H_{11})$_3$, H_2). ^{1}H NMR (300.08 MHz, THF-d_8, ppm): δ 1.31−2.87 (m, 66H, P(C_6H_{11})$_3$), 0.80 (t, $^2J_{(HP)}$ = 21 Hz, 2H, H_2). ^{13}C{^{1}H}-NMR (75.47 MHz, benzene-d_6, ppm): δ 36.5 (t, $J_{(PC)}$ = 12 Hz, P−C), 30.9, 30.3, 27.4, 26.6. ^{31}P{^{1} NMR (121.47 MHz, benzene-d_6, ppm): δ −4.93. Anal. Calcd for $C_{36}H_{68}I_2NOP_2Re$ (1032.89): C, 41.86; H, 6.64; N, 1.36. Found: C, 41.69; H, 6.56; N, 1.30. In comparison, the same reaction carried out in THF-d_8 afforded only 48% (**4a**) or 75% (**4b**) of the hydrogen coordinated product, which remained in an equilibrium with the starting material **3a**(**b**) at room temperature over 72 h.

T1 measurements were carried out at room temperature in benzene-d_6 at an NMR field strength of 11.7 T.

*4.2.5. [ReI$_2$(NO)(PR$_3$)$_2$(CO)] (**5**, R = iPr a, Cy b).* In a 3 mL Young-NMR-Tube, **3a** (17 mg, 0.02 mmol) or **3b** (21 mg, 0.02 mmol) was dissolved in 0.5 mL of benzene. The N_2 atmosphere was replaced with 1 bar of CO by using a freeze−pump−thaw cycle. After being kept at room temperature for 15 h, NMR spectroscopy indicated complete formation of the carbon monoxide coordinated rhenium diiodo complex **5a** or **5b** in 100% *in situ* yield. The mixture was filtered through a glass sintered funnel and the filtrate was dried *in vacuo*. The residue was washed with pentane (2 × 1 mL), dried affording a brown-yellow solid. **5a**: 13 mg, Yield: 79%. IR (ATR, cm^{-1}): ν(C−H) 2962, 2932, 2874, 1453, ν(CO) 1969, ν(NO) 1723. ^{1}H NMR (300.08 MHz, benzene-d_6, ppm): δ 3.00 (m, 6H, P-CH), 1.37−1.44 (m, 18 H, CH_3), 1.10−1.17 (m, 18 H, CH_3). ^{13}C{^{1}H}-NMR (75.47 MHz, $CDCl_3$, ppm): δ 26.65 (t, $J_{(PC)}$ = 12 Hz, P-CH), 21.05, 19.62. ^{31}P{^{1}H}-NMR (121.47 MHz, $CDCl_3$, ppm): δ −6.54 (s). Anal. Calcd for $C_{19}H_{42}I_2NO_2P_2Re$ (818.51): C, 27.88; H, 5.17; N, 1.71. Found: C, 27.54; H, 5.05; N, 1.70. **5b:** 12 mg, 56%. IR (ATR, cm^{-1}): ν(C−H) 2919, 2849, 1444, ν(CO) 1970, ν(NO) 1712. ^{1}H NMR (300.08 MHz, benzene-d_6, ppm): δ 1.22−2.92 (m, 66H, P(C_6H_{11})$_3$). ^{13}C{^{1}H}-NMR (75.47 MHz, $CDCl_3$, ppm): δ 37.00 (t, $J_{(PC)}$ = 11 Hz, P-CH), 31.24, 29.85, 27.76, 26.58. ^{31}P{^{1}H}-NMR (121.47 MHz, $CDCl_3$, ppm): δ −14.51 (s). Anal. Calcd for $C_{37}H_{66}I_2NO_2P_2Re$ (1058.89): C, 41.97; H, 6.28; N, 1.32. Found: C, 42.05; H, 6.55; N, 1.17. When the same reaction was investigated by NMR and IR within 5 min, formation of the carbonyl isomer **5′** was observed in quantitative yield. **5a′**: IR (ATR, cm^{-1}): ν(C−H) 2962, 2930, 2873, 1457, ν(CO) 2082, ν(NO) 1708. ^{1}H NMR (300.08 MHz, benzene-d_6, ppm): δ 3.15 (m, 6H, P-CH), 1.19−1.26 (m, 36 H, CH_3). ^{31}P{^{1}H}-NMR (121.47 MHz, $CDCl_3$, ppm): δ −16.67 (s). **5b′:** IR (ATR, cm^{-1}): ν(C−H) 2924, 2852, 1443, ν(CO) 2074, ν(NO) 1701. ^{1}H NMR (300.08 MHz, benzene-d_6, ppm): δ 1.29−3.21 (m, 66H, P(C_6H_{11})$_3$). ^{31}P{^{1}H}-NMR (121.47 MHz, $CDCl_3$, ppm): δ −26.29 (s).

*4.2.6. [R$_3$PH][HB(C$_6$F$_5$)$_3$] (**6**, R = iPr a, Cy b) Formed in the Catalytic Hydrogenation of 1-Hexene by the "[Re]/Hydrosilane/B(C$_6$F$_5$)$_3$" Reagent.* In a 30 mL steel autoclave equipped with a stirring bar, **3a** (4.5 mg, 0.0075 mmol), $B(C_6F_5)_3$ (10.4 mg, 0.02 mmol) and Et_3SiH (5.0 μL, 0.03 mmol) were dissolved in 2.5 mL 1-hexene. After charging with 10 bar of H_2, hydrogenation occurred and the catalysis was deliberately terminated by removing the H_2 atmosphere after 10 min corresponding to an approximate half conversion. Precipitates were observed in the reaction vessel and separated from the solution, dried *in vacuo*. **6a:** ^{1}H NMR (300.08 MHz, C_6D_5Cl, ppm): δ 5.62 (dxq, 1H, $^3J_{HH}$ = 4 Hz, $^1J_{HP}$ = 458 Hz, PH), 2.88 (m, 6H, PCH(CH_3)$_2$), 1.37−1.49 (m, 36H, PCH(CH_3)$_2$). ^{13}C{^{1}H}-NMR (75.47 MHz, C_6D_5Cl, ppm): δ 19.31, 18.79, 17.19, 17.15. ^{31}P{^{1}H}-NMR (121.47 MHz, C_6D_5Cl, ppm): δ 43.9 (s). ^{11}B NMR (96.28 MHz, C_6D_5Cl, ppm): δ −25.44 (d, $^1J_{HB}$ = 92 Hz). ^{19}F NMR (282.33 MHz, C_6D_5Cl, ppm): δ −133.40 (m, 6F, *ortho*-C_6F_5), −163.54 (t, $^1J_{CF}$ = 19 Hz, 3F, *para*-C_6F_5), −166.64 (m, 6F, *meta*-C_6F_5). MS (ESI): *m*/*z* 161.0 [*i*Pr$_3$PH]$^+$, 513.0 [HB(C_6F_5)$_3$]$^-$. This product was invariably observed in the resultant solution in each **3a** or **2a** catalyzed hydrogenation of 1-hexene. Similarly, the formation of **6b** was observed during the hydrogenation courses of the "**3b**/hydrosilane/B(C_6F_5)$_3$" catalytic system. For instance, the hydrogenation of 1-hexene (3 mL) with **3b** (40 mg, 0.04 mmol), Me_2PhSiH (16 μL, 0.10 mmol) and $B(C_6F_5)_3$ (41 mg, 0.08 mmol) under 10 bar of H_2 afforded a brown precipitate, from which colorless single crystals of **6b** were obtained from a layered solution of pentane and chlorobenzene. ^{1}H NMR (300.08 MHz, C_6D_5Cl, ppm): δ 4.80 (dxq, 1H, $^3J_{HH}$ = 4 Hz, $^1J_{HP}$ = 446 Hz, PH), 1.04−2.08 (m, 66H, P(C_6H_{11})$_3$). ^{13}C{^{1}H}-NMR (75.47 MHz, C_6D_5Cl, ppm): δ 171.47, 125.52, 46.72, 28.24, 26.70, 15.62. ^{31}P{^{1}H}-NMR (121.47 MHz, C_6D_5Cl, ppm): δ 32.9 (s). ^{11}B NMR (96.28 MHz, C_6D_5Cl, ppm): δ −27.29 (d, $^1J_{HB}$ = 69 Hz). ^{19}F NMR (282.33 MHz, C_6D_5Cl, ppm): δ −134.16 (m, 6F, *ortho*-C_6F_5), −164.93 (t, $^1J_{CF}$ = 21 Hz, 3F, *para*-C_6F_5), −167.95 (m, 6F, *meta*-C_6F_5). MS (ESI): *m*/*z* 281.2 [Cy_3PH]$^+$, 513.0 [HB(C_6F_5)$_3$]$^-$. Anal. Calcd for $C_{36}H_{35}BF_{15}P$ (794.42): C, 54.43, H, 4.44. Found: C, 54.51; H, 4.40.

4.2.7. Deuterium Isotope Effect of "3/Hydrosilane/B(C$_6$F$_5$)$_3$" Catalyzed Hydrogenation of 1-Hexene. In a 30 mL steel autoclave equipped with a stirring bar, rhenium complex (**3a**, 1.5 mg, 0.0025 mmol; **3b**, 2.0 mg, 0.0025 mmol), $B(C_6F_5)_3$ (5.2 mg, 0.01 mmol) and hydrosilane (Me_2PhSiH, 1.6 μL, 0.01 mmol; Et_3SiH, 1.6 μL, 0.01 mmol) were dissolved in 2.5 mL of 1-hexene. After being flushed with 3.7 bar of D_2 thrice, the system was charged with 10 bar of D_2 and kept stirring at ambient temperature. After the full conversion was achieved, the supernatant solution was separated from the precipitate and further identified by ^{2}H NMR spectroscopy as purely 1,2-hydrogenated product. $C_4H_9CHDCH_2D$: ^{2}H NMR (46.06 MHz, toluene, ppm): δ 2.11 (s, −CHD−), 1.70 (s, $-CH_2D$). The precipitate was isolated and further verified as [DP*i*Pr$_3$][HB(C_6F_5)$_3$]. ^{31}P{^{1}H}-NMR (121.47 MHz, THF-d_8, ppm): δ 41.5 (s). ^{11}B NMR (96.28 MHz, THF-d_8, ppm): δ −25.11 (d, $^1J_{HB}$ = 90 Hz).

4.2.8. H$_2$/D$_2$ Scrambling Experiments. In a 3 mL Young-NMR-tube, **3a** (4.5 mg, 0.006 mmol), $B(C_6F_5)_3$ (10.4 mg, 0.02 mmol) and Me_2PhSiH (3.2 μL, 0.02 mmol) were dissolved in 0.5 mL of toluene-d_8. The nitrogen atmosphere was replaced with 1100 mbar of H_2 and D_2 in a 1:1 ratio using a freeze−pump−thaw cycle. The solution was kept at 23 °C for 10 min, and was investigated by NMR spectroscopy showing the formation of HD along with **4a** and the phosphonium borate **6a**. ^{1}H NMR (199.95 MHz, toluene-d_8, ppm, 296 K): δ 4.41 (t, J = 43 Hz, HD), 4.51 (dxq, 1H, $^3J_{HH}$ = 4 Hz, $^1J_{HP}$ = 458 Hz, P−H). ^{31}P{^{1}H}-NMR (80.94 MHz, toluene-d_8, ppm): δ 42.2 (**6a**), 3.33 (**4a**).

*4.2.9. [ReI$_2$(**^{15}NO**)(PCy$_3$)$_2$(η^2-H$_2$)] (**4b-^{15}N**).* First the ^{15}N-enriched Re(II) precursor [NEt_4]$_2$[Re(^{15}NO)Br_5] was prepared according to reported procedure by passing ^{15}NO gas, which was produced from the reaction of $Na^{15}NO_2$ with $FeSO_4{\cdot}7H_2O$ and H_2O. 430 mg of the Re(II) precursor was obtained from 1 g of Re and 1 g of $Na^{15}NO_2$ which gives a low yield of ca. 10% due to the inefficient reaction of rhenium oxide with generated ^{15}NO. By following the synthetic procedure described for **3b** and **4b**, the fully ^{15}N enriched complex **4b-^{15}N** was prepared in an overall yield of 7%. ^{15}N NMR (50.69 MHz, toluene-d_8, ppm): δ −49.4 (t, $^2J_{NH}$ = 5 Hz).

*4.2.10. [ReI$_2$(H)(NO)(PCy$_3$)$_2$] (**7b**).* In a 3 mL Young-NMR-Tube, [$ReBr_2$(H)(NO)(PCy_3)$_2$] (65 mg, 0.07 mmol) and excess of NaI (230 mg, 1.53 mmol) were mixed in 2 mL of THF. The mixture was kept stirring at 23 °C for 15 h to afford a dark-brown solution. The mixture was filtered through a glass sintered funnel to remove the NaBr byproduct. The filtrate was dried *in vacuo* and further extracted with toluene (3 × 2 mL) and dried to afford the Re(II) diiodo hydride as a black-brown solid. Yield: 59 mg, 82%. IR (ATR, cm^{-1}): ν(C−H) 2921, 2855, 1437, ν(Re−H) 2006, ν(NO) 1684. Anal. Calcd for $C_{36}H_{67}I_2NOP_2Re$ (1031.89): C, 41.90; H, 6.54; N, 1.36. Found: C, 41.61; H, 6.79; N, 1.26.

*4.2.11. [ReI(H)(NO)(PCy$_3$)$_2$] (**8b**).* In a 20 mL vial in glovebox, **7b** (40 mg, 0.04 mmol) was treated with excess of zinc powder in THF solution and the mixture was kept stirring at 23 °C (Cautions: reaction at higher temperatures afforded only a complex mixture) for overnight to afford a dark-purple solution. The excess of zinc was removed by

dx.doi.org/10.1021/ja400135d | J. Am. Chem. Soc. 2013, 135, 4088−4102

filtration and the filtrate was dried *in vacuo*. The resulted brown residue was further extracted with pentane (5 × 2 mL) and dried *in vacuo* giving a purple solid. Yield: 18 mg, 52%. IR (ATR, cm^{-1}): ν(C−H) 2922, 2851, 1442, ν(NO) 1657. ^1H NMR (300.08 MHz, benzene-d_6, ppm): δ 1.25−2.79 (m, 66H, P(C_6H_{11})$_3$), −15.92 (br, 1H, Re−H). $^{13}C\{^1H\}$-NMR (75.47 MHz, benzene-d_6, ppm): δ 31.28, 30.66, 28.22, 27.05. $^{31}P\{^1H\}$-NMR (121.47 MHz, benzene-d_6, ppm): δ 31.2 (s). Anal. Calcd for $C_{36}H_{67}INOP_2Re$ (904.98): C, 47.78; H, 7.46; N, 1.55. Found: C, 47.51; H, 7.40; N, 1.51.

4.3. Computational Details. All calculations were carried out with the TURBOMOLE 6.3 suite of programs.[33] The structures were optimized with the *meta*-GGA functional TPSS[12] applying the D3-dispersion correction with Becke-Johnson damping.[14] Subsequent single-point calculations were carried out at the more accurate double-hybrid density functional B2PLYP-D3 level.[15] For both calculations the large Gaussian-AO basis set def2-TZVP[13] and the RI approximation[34] were used. The final level of theory can therefore be abbreviated as B2PLYP-D3/def2-TZVP//TPSS-D3/def2-TZVP and has an estimated accuracy of about 1−2 kcal/mol. Further details can be found in the Supporting Information.

4.4. X-ray Diffraction Analyses. Single-crystal X-ray diffraction data were collected at 183(2) K on a Xcalibur diffractometer (Agilent Technologies, Ruby CCD detector) for all compounds using a single wavelength Enhance X-ray source with MoKα radiation (λ= 0.71073 Å).[35] The selected suitable single crystals were mounted using polybutene oil on the top of a glass fiber fixed on a goniometer head and immediately transferred to the diffractometer. Pre-experiment, data collection, data reduction and analytical absorption corrections[36] were performed with the program suite *CrysAlis^{Pro}*.[35] The crystal structures were solved with SHELXS97[35] using direct methods. The structure refinements were performed by full-matrix least-squares on F^2 with SHELXL97.[37] All programs used during the crystal structure determination process are included in the WINGX software.[38] PLATON[39] was used to check the result of the X-ray analyses. For more details, see the Crystallographic Information files (Supporting Information). CCDC-907258 (for **2a**), CCDC-907259 (for **3b**), CCDC-907260 (for **5b**), CCDC-907261 (for **6b**), and CCDC-907262 (for **7b**) contain the supplementary crystallographic data (excluding structure factors) for this paper. These data can be obtained free of charge from The Cambridge Crystallographic Data Centre via www.ccdc.cam.ac.uk/data_request/cif.

■ ASSOCIATED CONTENT

Ⓢ Supporting Information

Experimental Section with detailed synthesis and characterization of complexes, the crystallographic details of **2a**, **3b**, **5b**, **6b** and **7b**, various ^1H-, ^{13}C-, ^{31}P-, ^{19}F-, ^{29}Si- and ^{15}N NMR spectra, representative hydrogenation profiles, the figure of transformation course from **5a′** to **5a**, further computational details and additional numbers and structures. Crystallographic information files. This material is available free of charge via the Internet at http://pubs.acs.org.

■ AUTHOR INFORMATION

Corresponding Author

hberke@aci.uzh.ch

Notes

The authors declare no competing financial interest.

■ ACKNOWLEDGMENTS

Financial support from the Swiss National Science Foundation, Lanxess AG, Leverkusen, Germany, the Funds of the University of Zurich, the DFG and SNF within the project 'Forschergruppe 1175 - Unconventional Approaches to the Activation of Dihydrogen' are gratefully acknowledged.

■ REFERENCES

(1) (a) Richter-Addo., G. B.; Legzdins, P. *Metal Nitrosyls*; Oxford University Press: New York, 1992; (b) Hayton, T. W.; Legzdins, P.; Sharp, W. B. *Chem. Rev.* **2002**, *102*, 935. (c) Richter-Addo, G. B.; Legzdins, P.; Burstyn, J. *Chem. Rev.* **2002**, *102*, 857. (d) Roncaroli, F.; Videla, M.; Slep, L. D.; Olabe, J. A. *Coord. Chem. Rev.* **2007**, *251*, 1903. (e) Coppens, P.; Novozhilova, I.; Kovalevsky, A. *Chem. Rev.* **2002**, *102*, 861. (f) Machura, B. *Coord. Chem. Rev.* **2005**, *249*, 2277.

(2) (a) Enemark, J. H.; Feltham, R. D. *Coord. Chem. Rev.* **1974**, *13*, 339. (b) Enemark, J. H.; Feltham, R. D. *Top. Stereochem.* **1981**, *12*, 155. (c) Song, J.; Hall, M. B. *J. Am. Chem. Soc.* **1993**, *115*, 327. (d) Ogasawara, M.; Huang, D.; Streib, W. E.; Huffman, J. C.; Gallego-Planas, N.; Maseras, F.; Eisenstein, O.; Caulton, K. G. *J. Am. Chem. Soc.* **1997**, *119*, 8642. (e) Hodgson, D. J.; Payne, N. C.; McGinnety, J. A.; Pearson, R. G.; Ibers, J. A. *J. Am. Chem. Soc.* **1968**, *90*, 4486. (f) Pierpont, C. G.; Van Derveer, D. G.; Durlang, W.; Eisenberg, R. *J. Am. Chem. Soc.* **1970**, *92*, 4760. (g) Colman, J. P.; Farnham, P. H.; Dolcetti, G. *J. Am. Chem. Soc.* **1971**, *93*, 1788.

(3) Enemark, J. H.; Feltham, R. D. *Proc. Natl. Acad. Sci. U.S.A.* **1972**, *69*, 3534.

(4) (a) Llamazares, A.; Schmalle, H. W.; Berke, H. *Organometallics* **2001**, *20*, 5277. (b) Gusev, D.; Llamazares, A.; Artus, G.; Jacobsen, H.; Berke, H. *Organometallics* **1999**, *18*, 75. (c) Bohmer, J.; Haselhorst, G.; Wieghart, K.; Nuber, B. *Angew. Chem., Int. Ed. Engl.* **1994**, *13*, 1473. (d) Legzdins, P.; Sayers, S. F. *Chem.—Eur. J.* **1997**, *3*, 1579. (e) Crease, A. E.; Legzdins, P. *Chem. Commun.* **1972**, 268. (f) Crease, A. e.; Legzdins, P. *Dalton Trans.* **1973**, 1501. (g) Lee, K. E.; Arif, A. M.; Gladysz, J. A. *Chem. Ber.* **1991**, *124*, 309. (h) Sharp, W. B.; Legzdins, P.; Patrick, B. O. *J. Am. Chem. Soc.* **2001**, *123*, 8143.

(5) Negishi, E. *Chem.—Eur. J.* **1999**, *5*, 411.

(6) (a) de Vries, J. G.; Elsevier, C. J. *The Handbook of Homogeneous Hydrogenation*; Wiley-VCH: Weinheim, 2007; For selective examples: (b) Crabtree, R. H. *Acc. Chem. Res.* **1979**, *12*, 331. (c) Osborn, J. A.; Jardine, F. H.; Young, J. F.; Wilkinson, G. *J. Chem. Soc. A.* **1966**, *12*, 1711. (d) Schrock, R. R.; Osborn, J. A. *J. Am. Chem. Soc.* **1976**, *98*, 2134. (e) Schrock, R. R.; Osborn, J. A. *J. Am. Chem. Soc.* **1976**, *98*, 4450. (f) Landis, C. R.; Halpern, J. *J. Am. Chem. Soc.* **1987**, *109*, 1746. (g) Helmchen, G.; Pfaltz, A. *Acc. Chem. Res.* **2000**, *6*, 336. (h) Roseblade, S. J.; Pfaltz, A. *Acc. Chem. Res.* **2007**, *12*, 1402. (i) Yi, C. S.; Lee, D. W. *Organometallics* **1999**, *18*, 5152. (j) Noyori, R.; Hashiguchi, S. *Acc. Chem. Res.* **1997**, *30*, 97.

(7) (a) Dudle, B.; Rajesh, K.; Blacque, O.; Berke, H. *J. Am. Chem. Soc.* **2011**, *133*, 8168. (b) Jiang, Y.; Blacque, O.; Fox, T.; Frech, C. M.; Berke, H. *Organometallics* **2009**, *28*, 5493. (c) Choualeb, A.; Maccaroni, E.; Blacque, O.; Schmalle, H. W.; Berke, H. *Organometallics* **2008**, *27*, 3474. (d) Jiang, Y.; Berke, H. *Chem. Commun.* **2007**, 3571. (e) Landwehr, A.; Dudle, B.; Fox, T.; Blacque, O.; Berke, H. *Chem.—Eur. J.* **2012**, *18*, 5701.

(8) Jiang, Y.; Hess, J.; Fox, T.; Berke, H. *J. Am. Chem. Soc.* **2010**, *132*, 18233.

(9) (a) Pauling, L. *Science* **1994**, *263*, 983. (b) Kim, K. C.; Reed, C. A.; Elliott, D. W.; Mueller, L. J.; Tham, F.; Lin, L.; Lambert, J. *Science* **2002**, *297*, 825. (c) Ree, C. A. *Acc. Chem. Res.* **1998**, *31*, 325. (d) Reed, C. A. *Acc. Chem. Res.* **2010**, *43*, 121.

(10) (a) Blackwell, J. M.; Sonmor, E. R.; Scoccitti, T.; Piers, W. E. *Org. Lett.* **2000**, *2*, 3921. (b) Parks, D. J.; Blackwell, J. M.; Piers, W. E. *J. Org. Chem.* **2000**, *65*, 3090. (c) Berkefeld, A.; Piers, W. E.; Parvez, M. *J. Am. Chem. Soc.* **2010**, *132*, 10660.

(11) (a) Rendler, S.; Oestreich, M. *Angew. Chem., Int. Ed.* **2008**, *47*, 5997. (b) Hog, D. T.; Oestreich, M. *Eur. J. Org. Chem.* **2009**, 5047. (c) Klare, H. F. T.; Oestreich, M.; Ito, J.-i.; Nishiyama, H.; Ohki, Y.; Tatsumi, K. *J. Am. Chem. Soc.* **2011**, *133*, 3312. (d) Mewald, M.; Froehlich, R.; Oestreich, M. *Chem.—Eur. J.* **2011**, *17*, 9406. (e) Muether, K.; Froehlich, R.; Mueck-Lichtenfeld, C.; Grimme, S.; Oestreich, M. *J. Am. Chem. Soc.* **2011**, *133*, 12442.

(12) Tao, J.; Perdew, J. P.; Staroverov, V. N.; Scuseria, G. E. *Phys. Rev. Lett.* **2003**, *91*, 146401.

(13) Weigend, F.; Ahlrichs, R. *Phys. Chem. Chem. Phys.* **2005**, *7*, 3297.

(14) (a) Grimme, S.; Antony, J.; Ehrlich, S.; Krieg, H. *J. Chem. Phys.* **2010**, *132*, 154104. (b) Grimme, S.; Ehrlich, S.; Goerigk, L. *J. Comput. Chem.* **2011**, *32*, 1456.
(15) (a) Grimme, S. *J. Chem. Phys.* **2006**, *124*, 034108. (b) Schwabe, T.; Grimme, S. *Phys. Chem. Chem. Phys.* **2006**, *8*, 4398.
(16) (a) Kubas, G. J. *Chem. Rev.* **2007**, *107*, 4152. (b) Kubas, G. J. *Metal Dihydrogen and σ-Bond Complexes*; Kluwer: New York, 2001; (c) Kubas, G. J. *Acc. Chem. Rev.* **1988**, *21*, 120. (d) Kubas, G. J.; Ryan, R. R.; Swanson, B. I.; Vergamini, P. J.; Wasserman, H. J. *J. Am. Chem. Soc.* **1984**, *106*, 451. (e) Hoffmann, R. *Am. Sci.* **2012**, 374. (f) Berke, H. *ChemPhysChem* **2011**, *9*, 1837.
(17) Matthews, S. L.; Heinekey, D. M. *J. Am. Chem. Soc.* **2006**, *128*, 2615.
(18) (a) Balcells, D.; Carbo, J. J.; Maseras, F.; Eisenstein, O. *Organometallics* **2004**, *23*, 6008. (b) Huang, D.; Streib, W. E.; Eisenstein, O.; Kenneth, K. G. *Organometallics* **2000**, *19*, 1967.
(19) Mayr, H.; Basso, N.; Hagen, G. *J. Am. Chem. Soc.* **1992**, *114*, 3060.
(20) Welch, G. C.; Cabrera, L.; Chase, P. A.; Hollink, E.; Masuda, J. D.; Wei, P. R.; Stephan, D. W. *Dalton Trans.* **2007**, 3407.
(21) (a) Stephan, D. W.; Erker, G. *Angew. Chem., Int. Ed.* **2010**, *49*, 46. (b) Stephan, D. W. *Org. Biomol. Chem.* **2008**, *6*, 1535. (c) Stephan, D. W. *Dalton Trans.* **2009**, 3129. (d) Chase, P. A.; Stephan, D. W. *Angew. Chem., Int. Ed.* **2008**, *47*, 7433. (e) Kenward, A. L.; Piers, W. E. *Angew. Chem., Int. Ed.* **2008**, *47*, 38. (f) Welch, G. C.; Juan, R. R. S.; Masuda, J. D.; Stephan, D. W. *Science* **2006**, *314*, 1124. (g) Spies, P.; Schwendemann, S.; Lange, S.; Kehr, G.; Frohlich, R.; Erker, G. *Angew. Chem., Int. Ed.* **2008**, *47*, 7543.
(22) (a) Ingleson, M. J.; Brayshaw, S. K.; Mahon, M. F.; Ruggiero, G. D.; Weller, A. S. *Inorg. Chem.* **2005**, *44*, 3162. (b) Kubas, G. J. *Adv. Inorg. Chem.* **2004**, *56*, 127. (c) Yi, C. S.; Lee, D. W.; He, Z.; Rheingold, A. L.; Lam, K.-C.; Concolino, T. E. *Organometallics* **2000**, *19*, 2909.
(23) (a) Parkin, G. *Acc. Chem. Res.* **2009**, *42*, 315. (b) Iuliis, M. Z. D.; Morris, R. H. *J. Am. Chem. Soc.* **2009**, *131*, 11263. (c) Jones, W. D. *Acc. Chem. Res.* **2002**, *36*, 140. (d) Gould, G. L.; Heinekey, D. M. *J. Am. Chem. Soc.* **1989**, *111*, 5502.
(24) Marsmann, H.; Uhlig, F.; Mikhova, B. *Chemical Shifts and Coupling Constants for Silicon-29*, Springer: Berlin, Heidelberg, New York, 2008.
(25) Mason, J.; Larkworthy, L. F.; Moore, E. A. *Chem. Rev.* **2002**, *102*, 913.
(26) (a) Berger, S.; Braun, S.; Kalinowski, H. O. *NMR-Spektroskopie von Nichtmetallen*; Georg Thieme Verlag: Stuttgart, NY, 1992. (b) Bell, L. K.; Mason, J.; Mingos, D. M. P.; Tew, D. G. *Inorg. Chem.* **1983**, *22*, 3497. (c) Botto, R. E.; Kolthammer, B. W. S.; Legzdins, P.; Roberts, J. D. *Inorg. Chem.* **1979**, *18*, 2049. For other examples with high δ_N: (d) Gaviglio, C.; Ben-David, Y.; Shimon, L. J. W.; Doctorovich, F.; Milstein, D. *Organometallics* **2009**, *28*, 1917. (e) Duffin, P. A.; Larkworthy, L. F.; Mason, J.; Stephens, A. N.; Thompson, R. M. *Inorg. Chem.* **1987**, *26*, 2034. (f) Evans, D. H.; Mingos, D. M. P.; Mason, J.; Richards, A. *J. Organomet. Chem.* **1983**, *249*, 293.
(27) (a) Jessop, P. G.; Morris, R. H. *Coord. Chem. Rev.* **1992**, 155. (b) Jia, G.; Morris, R. H. *J. Am. Chem. Soc.* **1991**, *113*, 875. (c) Jia, G.; Lough, A. J.; Morris, R. H. *Organometallics* **1992**, *1*, 161. (d) Cappellani, E. P.; Drouin, S. D.; Jia, G. C.; Maltby, P. A.; Morris, R. H.; Schweitzer, C. T. *J. Am. Chem. Soc.* **1994**, *116*, 3375.
(28) Li, T.; Lough, A. J.; Morris, R. H. *Chem.—Eur. J.* **2007**, *13*, 3796.
(29) (a) Noyori, R.; Ohkuma, T. *Angew. Chem., Int. Ed.* **2001**, *40*, 40. (b) Noyori, R.; Yamakawa, M.; Hashiguchi, S. *J. Org. Chem.* **2001**, *66*, 7931. (c) Morris, R. H. *Chem. Soc. Rev.* **2009**, *38*, 2282. (d) Abdur-Rashid, K.; Clapham, S. E.; Hadzovic, A.; Harvey, J. N.; Lough, A. J.; Morris, R. H. *J. Am. Chem. Soc.* **2002**, *124*, 15104. (e) Morris, R. H. *Coord. Chem. Rev.* **2008**, *252*, 2381. (f) Clapham, S. E.; Hadzovic, A.; Morris, R. H. *Coord. Chem. Rev.* **2004**, *248*, 2201. (g) Maire, P.; Buettner, T.; Breher, F.; Le Floch, P.; Gruetzmacher, H. *Angew. Chem., Int. Ed.* **2005**, *44*, 6318.
(30) For an excellent highlight on cooperating ligands in catalysis, see: Gruetzmacher, H. *Angew. Chem., Int. Ed.* **2008**, *47*, 1814. For an excellent perspective on redox non-innocent ligands, see: Lyaskovskyy, V.; de Bruin, B. *ACS Catal.* **2012**, *2*, 270.
(31) Clayden, J.; Greeves, N.; Warren, S.; Wothers, P. *Organic Chemistry*; Oxford University Press: New York, 2001.
(32) Jiang, Y.; Blacque, O.; Fox, T.; Frech, C. M.; Berke, H. *Chem.—Eur. J.* **2010**, *16*, 2240.
(33) Ahlrichs, R.; Armbruster, M. K.; Baer, M.; Baron, H.-P.; Bauernschmitt, R.; Crawford, N.; Deglmann, P.; Ehrig, M.; Eichkorn, K.; Elliott, S.; Furche, F.; Haase, F.; Haeser, M.; Haettig, C.; Hellweg, A.; Horn, H.; Huber, C.; Huniar, U.; Kattannek, M.; Koelmel, C.; Kollwitz, M.; May, K.; Nava, P.; Ochsenfeld, C.; Oehm, H.; Patzelt, H.; Rappoport, D.; Rubner, O.; Schaefer, A.; Schneider, U.; Sierka, M.; Treutler, O.; Unterreiner, B.; von Arnim, M.; Weigand, F.; Weis, P.; *TURBOMOLE*, 2008, http://www.turbomole.com.
(34) (a) Eichkorn, K.; Treutler, O.; Öhm, H.; Häser, M.; Ahlrichs, R. *Chem. Phys. Lett.* **1995**, *240*, 283. (b) Hättig, C.; Weigend, F. *J. Chem. Phys.* **2000**, *113*, 5154.
(35) Agilent Technologies (formerly Oxford Diffraction), Yarnton, England, 2011.
(36) Clark, R. C.; Reid, J. S. *Acta Crystallogr., Sect. A* **1995**, *51*, 887.
(37) Sheldrick, G. M. *Acta Crystallogr., Sect. A* **2008**, 64.
(38) Farrugia, L. J. *J. Appl. Crystallogr.* **1999**, *32*, 837.
(39) Spek, A. L. *J. Appl. Crystallogr.* **2003**, *36*, 7.